

**Observations and
identification of a novel
population of parietal ridge
osteoprogenitor stem cells
in a rat critical-sized
calvarial defect bone
regeneration model**

by

Richard B. Hill, DDS

Thesis submitted to the Faculty of the
Oral Biology Graduate Program
Uniformed Services University of the Health Sciences
In partial fulfillment of the requirements for the degree of
Master of Science 2019

DISSERTATION APPROVAL SHEET

Observations and identification of a novel population of parietal ridge osteoprogenitor stem cells in a rat critical-sized calvarial defect bone regeneration model

This thesis is submitted by Richard B. Hill and has been examined and approved by an appointed committee of the faculty of the Uniformed Services University of the Health Sciences.

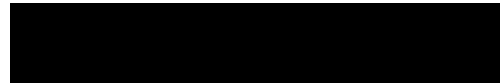
The signatures that appear below verify the fact that all required changes have been incorporated and that the thesis has received final approval with reference to content, form and accuracy of presentation.

This thesis is therefore in partial fulfillment of the requirements for the degree of Master of Science.

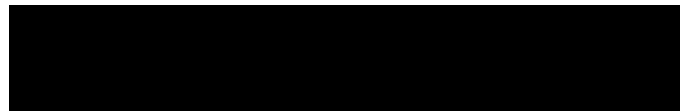
04 June 2019
Date



Major Advisor ✓



Department Chairperson ✓

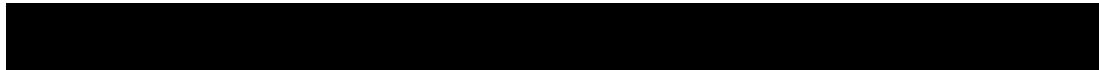


Dean, School of Graduate Studies

"Observations and identification of a novel population of parietal ridge osteoprogenitor stem cells in a rat critical-sized calvarial defect bone regeneration model"

CPT Richard Hill

APPROVED:

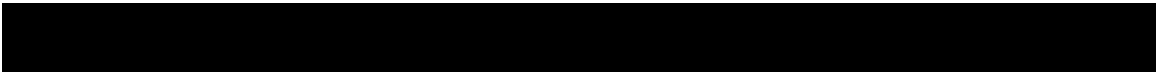


KENNETH J. ERLEY, COL, DMD, PROGRAM DIRECTOR

17 May 2019

DATE

APPROVED:



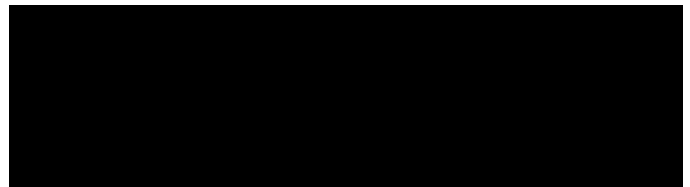
PETER GUEVARA, COL, DMD
DEAN, ARMY POST-GRADUATE DENTAL SCHOOL

“The author hereby certifies that the use of any copyrighted material in the thesis/dissertation manuscript entitled:

“Observations and identification of a novel population of parietal ridge osteoprogenitor stem cells in a rat critical-sized calvarial defect bone regeneration model”

is appropriately acknowledged and, beyond brief excerpts, is with the permission of the copyright owner.

CPT Richard B Hill, DDS
US Army Periodontics
Uniformed Services University
07 MAY 2019



Distribution Statement

Distribution A: Public Release.

The views presented here are those of the author and are not to be construed as official or reflecting the views of the Uniformed Services University of the Health Sciences, the Department of Defense or the U.S. Government.

ACKNOWLEDGEMENTS

I would like to thank the members of the committee (Drs. Erley, Johnson, Herold, O'Bryhim) for their instruction, feedback and support in accomplishing this goal. Additionally, I would like to thank my co-resident, Dr. Ryan McGary, for being the perfect laboratory teammate.

DEDICATION

To my wife Maya without whom nothing is possible.

COPYRIGHT STATEMENT

The author hereby certifies that the use of any copyrighted material in the thesis manuscript entitled: “Observations and identification of a novel population of parietal ridge osteoprogenitor stem cells in a rat critical-sized calvarial defect bone regeneration model” is appropriately acknowledged and, beyond brief excerpts, is with the permission of the copyright owner.

Richard Hill

Richard B. Hill

08 APR 2019

ABSTRACT

“Observations and identification of a novel population of parietal ridge osteoprogenitor stem cells in a rat critical-sized calvarial defect bone regeneration model”

Richard B. Hill, DDS, 2019

Thesis directed by: COL Kenneth J. Erley, LTC Thomas M. Johnson

It has been previously observed that, after creation of a critical-sized calvarial defect, a rat model exhibits bone healing initiation from two distinct foci: the underlying dura mater and the adjacent parietal ridge bone eminence. During healing, distinct islands of cartilage appear in the dural region but do not appear near the parietal ridge. This study utilized immunohistochemistry to investigate how stem/osteoprogenitor cells in the parietal ridge region differed in their healing response in the presence of varying concentrations of recombinant human bone morphogenetic protein-2. Response to the markers used was observed to be different in the two regions of interest. These data support that the stem/osteoprogenitor cells within these two regions represent distinct subtypes not previously identified.

TABLE OF CONTENTS

DISSERTATION APPROVAL SHEET	ii
ACKNOWLEDGEMENTS	iii
DEDICATION	iv
COPYRIGHT STATEMENT	v
ABSTRACT	vi
TABLE OF CONTENTS	vii
LIST OF TABLES	ix
LIST OF FIGURES	ix
LIST OF ABBREVIATIONS	xi
INTRODUCTION	1
STATEMENT OF THE PROBLEM.....	1
SIGNIFICANCE	2
REVIEW OF THE LITERATURE	3
INTRODUCTION	3
Critical-Sized Bone Defects.....	4
Stem/progenitor cells and differentiation in bone.....	5
BONE DEVELOPMENT AND HEALING	7
Bone Structure: Cortical and Trabecular Bone	7
Formation	8
Bone Eminences	9
Rat Calvarial Defects.....	9
Mechanisms Of Bone Healing.....	10
HYPOXIA AND STEM CELL ACTIVATION	11
Macrophages.....	12
IMMUNOHISTOCHEMISTRY	13
IMMUNOFLUORESCENCE.....	15
Available Candidate Stem Cell Markers	16
SUMMARY	16
PURPOSE	17
HYPOTHESES	18
HYPOTHESIS #1	18
HYPOTHESIS #2	18
HYPOTHESIS #3	18
SPECIFIC AIMS	19
AIM #1	19
AIM #2	19
AIM #3	20
MATERIALS AND METHODS	21
OVERVIEW	21
SURGICAL PROCEDURE AND MATERIALS	21
CURRENT STUDY	22
DETAILED METHODOLOGY	24
Immunohistochemistry “Standard” Protocol.....	24

Immunofluorescence Protocol	25
RESTATEMENT OF HYPOTHESIS #1: Stem/progenitor cells.....	27
Anticipated Results.....	27
Graphical Depiction of Results	28
RESTATEMENT OF THE HYPOTHESIS #2: HIF-1 and SDF-1	28
Detailed Methodology.....	29
Anticipated Results.....	29
Graphical Depiction of Results	29
RESTATEMENT OF THE HYPOTHESIS #3: M2 Macrophages.....	30
Detailed Methodology.....	30
Anticipated Results.....	30
Graphical Depiction of Results	31
INDEPENDENT VARIABLES	31
DEPENDENT VARIABLE	31
DATA ANALYSIS.....	32
RESULTS	33
Krüppel-like factor 4 (KLF-4).....	33
RNA-binding Protein Musashi Homolog 1 (Msi1).....	42
Sex Determining Region Y-Box 2 (SOX-2)	52
Proliferating Cell Nuclear Antigen (PCNA).....	57
Scleraxis Homolog A (SCXA).....	62
Sex Determining Region Y-Box 9 (SOX9)	67
DISCUSSION	70
FUTURE STUDIES	74
REFERENCES.....	75

LIST OF TABLES

LIST OF FIGURES

Figure

Flowchart

1. Cell Proliferation
2. HIF-1 and SDF-1 expression
3. Klf4 and CD68 expression
4. KLF-4 Day1 0 μ g rhBMP-2 1.10-6, 20X
5. KLF-4 Day1 5 μ g rhBMP-2 1.8-15, 20x
6. KLF-4 Day1 20 μ g rhBMP-2 1.25-14, 20x
7. KLF-4 Day3 0 μ g rhBMP-2 3.37-14, 20x
8. KLF-4 Day3 5 μ g rhBMP-2 3.32-9, 20x
9. KLF-4 Day3 20 μ g rhBMP-2 3.39-9, 20x
10. KLF-4 Day5 0 μ g rhBMP-2 5.103-2, 20x
11. KLF-4 Day5 5 μ g rhBMP-2 5.95-4, 20x
12. KLF-4 Day5 20 μ g rhBMP-2 5.90-15, 20x
13. KLF-4 Day7 0 μ g rhBMP-2 7.131-7, 20x
14. KLF-4 Day7 5 μ g rhBMP-2 7.126-15, 20x
15. KLF-4 Day7 20 μ g rhBMP-2 7.127-3 20x
16. KLF-4 Day14 0 μ g rhBMP-2 14.70-4, 20x
17. KLF-4 Day14 5 μ g rhBMP-2 14.71-13, 20x
18. KLF-4 Day14 20 μ g rhBMP-2 14.63-5 20x
19. Msi1 Day1 0 μ g rhBMP-2 1.4-8, 40x
20. Msi Day1 5 μ g rhBMP-2 1.2-6, 20x
21. Msi Day1 20 μ g rhBMP-2 1.3-6, 20x
22. Msi1 Day3 0 μ g 3.28-11, 40x
23. Msi1 Day3 5 μ g 3.29-11, 4x
24. Msi1 Day3 20 μ g 3.33-9, 20x
25. Msi1 Day5 0 μ g 5.82-13, 20x
26. Msi1 Day5 5 μ g 5.104-7, 20x
27. Msi1 Day5 20 μ g 5.84-13, 20x
28. Msi1 Day7 0 μ g 7.110-8, 4x
29. Msi1 Day7 5 μ g 7.111-6, 20x
30. Msi1 Day7 20 μ g 7.133-14, 20x
31. Msi1 Day14 0 μ g 14.61-12, 4x
32. Msi1 Day14 5 μ g 14.65-9, 20x
33. Msi1 Day14 20 μ g 14.62-5, 20x
34. SOX2 Day1 0 μ g 1.1-15, 4x
35. SOX2 Day1 0 μ g 1.1-15, 20x (Epidermis)
36. SOX2 Day1 0 μ g 1.1-15, 20x (Condyle)
37. SOX2 Day1 0 μ g 1.1-15, 20x
38. SOX2 Day3 0 μ g 3.46-6, 20x
39. SOX2 Day3 20 μ g 3.45-5, 20x

40. SOX2 Day7 0 μ g 7.131-3, 0 μ g 20x
41. SOX2 Day14-5 μ g 14.59-2, 20x
42. PCNA Day1 0 μ g 1.10-14 4x
43. PCNA Day1 5 μ g 1.8-8 20x
44. PCNA Day3 5 μ g 3.32-10 20
45. PCNA Day5 0 μ g 5.103-5 20x
46. PCNA Day7 5 μ g 7.129-15 20x
47. PCNA Day7 5 μ g 7.129-15 40x
48. PCNA Day14 5 μ g 14.71-5 20x
49. PCNA Day1 μ g 1.10-14 20x
50. SCXA Day1 20 μ g 1,25-15, 20x (Condyle)
51. SCXA Day1 0 μ g 1.10-3
52. SCXA Day3 0 μ g 3.37-15, 4x
53. SCXA Day3 5 μ g 3.32-6, 20x
54. SCXA Day5 20 μ g 5.90-14, 20x
55. SCXA Day5 20 μ g 5.90-14, 20x
56. SCXA Day7 0 μ g 7.131-6, 4x
57. SCXA Day7 20 μ g 7.127-4, 4x
58. SCXA Day14 0 μ g 14.70-5, 20x
59. SCXA Day14 20 μ g 14.63-6, 20x
60. SOX9 Day1 20 μ g 1.25-10, 20x
61. SOX9 Day1 20 μ g 1,25-10, 20x
62. SOX9 Day7 5 μ g 7,127-7, 40x (Dura)

LIST OF ABBREVIATIONS

IF:	Immunofluorescence
IHC:	Immunohistochemistry
Klf4:	Krüppel-like factor 4
Msi1:	RNA-binding protein musashi homolog 1
MSC:	Mesenchymal stem cells
PCNA:	Proliferating cell nuclear antigen
rhBMP-2:	Recombinant human bone morphogenetic protein-2
SOX9:	Sex determining region Y-Box 9
SOX2:	Sex determining region Y-Box 2
SCXA:	Scleraxis homolog A

INTRODUCTION

STATEMENT OF THE PROBLEM

Functional healing of bone following injury requires the formation of new bone tissue by osteoblast cells, which are in turn formed by differentiation of stem/progenitor cells accumulated at the site of injury. The behavior of stem/progenitor cells in bone during healing of pathologic or traumatic lesions is not well-understood, although it is known that stem/progenitor cells with osteoblastic and chondroblastic potential lie dormant in bone and the surrounding periosteum, and that these cells can be activated through injury and induced by signaling processes to proliferate and differentiate into osteoblasts that synthesize new tissue.

Current therapies targeting bone cells with a view to enhancing this process typically involve application of one or more growth factors, such as bone morphogenetic protein-2 (BMP-2), which may recruit stem/progenitor cells and induce resident bone cells to become more active in bone formation. The extent to which this occurs can be very important in determining the success or failure of the procedure. If stem/progenitor cells present in the tissue can be encouraged to proliferate and differentiate, and if this process can be sustained, then defect healing time and volume of fill may be achieved more predictably.

There are various cell populations in skeletal tissue that are potential targets for signaling systems to promote bone formation following injury. Proliferative osteogenic cells originating from the parietal ridge region of the rat calvarium have been observed populating regions of surgically created rat

critical-sized calvarial defects [O'Bryhim (2015), DeCardona (2015), Jusino (2015): Masters Theses]. Preliminary data suggest these cells appear to originate from stem/progenitor cells that are distinct from a population in the dura, and that they respond differently to BMP-2. Currently, the exact source and characteristics of these cells, and their relationship to other osteogenic cell populations, have not been established. Furthermore, the signals activating these cells remain to be determined.

Two potential signals generated during wound healing that could activate these cells are hypoxia, and protein factors released by inflammatory cells such as macrophages. However, the roles of these signaling systems remain to be determined, and the temporospatial organization of stem/progenitor cells and these signaling systems is unknown. Collectively, our lack of understanding of the mechanistic biology of bone regeneration limits our ability to take a rational approach to developing and improving clinical treatment strategies by exploiting underlying regulatory mechanisms.

SIGNIFICANCE

A deeper understanding of the biological mechanisms underlying bone regeneration would provide the basis for a rational approach to utilizing the inherent regenerative capabilities of local cells to promote reliable and quantitative healing of damaged bone and differentiation, leading to decreased healing time and more predictable results.

Military readiness depends on soldiers healing from their treatment quickly and allowing them to return earlier to their duty. By being able to regrow adequate bone predictably as part of an overall treatment plan, practitioners would be able to be more successful in their efforts.

REVIEW OF THE LITERATURE

INTRODUCTION

Although the head itself represents only 12% of the total body surface area, craniofacial injuries - often involving damage to bone - account for one third of all emergency room visits (Sethi, 2014). Combined with the myriad of developmental and cosmetic defects treated each year, there is a significant demand for clinical techniques that provide high-quality, reliable bone healing, particularly when bone tissue has been lost or removed, thereby creating a large defect.

Ideally, treatment would induce healing by regeneration of bone. In regenerative healing, lost tissues or bodily structures are completely replaced in a way that appears identical to the initial presentation. Regeneration, even of whole, limbs, is seen in amphibians and some other animals, indicating it is biologically feasible. However, this process is not common in mammals, even with application of current treatment strategies. Although mammalian bone has some regenerative capacity, many clinical defects exceed this capacity, and instead heal mostly by repair. This reparative process includes some regenerative events, but typically results in scar formation and some loss of structure and/or function. This produces a tissue or structure which has some

resemblance to the original presentation, but often with some measurable loss of function (Kumar, 2005). Thus, bone repair and regeneration are distinctly different processes and present with different cellular mechanisms and signaling pathways.

As yet, the regulatory mechanisms and cellular processes that govern the decision between regeneration and repair remain unknown. Although the biology of bone development and healing has been studied widely, many questions remain unanswered regarding how the involved cells signal one another to proliferate and differentiate in response to growth or repair stimuli.

Critical-Sized Bone Defects

Bone has an innate ability to regenerate to a certain modest extent before some inherent biological limitation is reached. Defects resulting from trauma, surgery or disease are restored to approximately their original condition unless the defect proves to extend beyond this biological limit. Thus, the cellular and molecular machinery for regeneration are already in place, and from observations of healing, they recapitulate some of the cellular and molecular pathways utilized during bone development.

Critical-size defects are those which cannot heal fully without intervention, either surgically or otherwise. That is, the size of the defect exceeds the innate regenerative capacity of the cellular machinery. For quite some time, autologous bone grafting has been considered the gold standard for surgical repair of critical-size defects. In this technique, additional resources are in effect grafted from

another location so the site is no longer critical-sized. However, it has many limitations including increased morbidity and lack of adequate donor tissue. Various substances and materials have been developed to make up for the limitations of autologous bone but have many limitations of their own, including graft infection, deleterious immune response and transmission of disease (Chenard, 2012).

Clinically, the ideal treatment would be to extend and sustain the regenerative capability of bone in a predictable manner. Induction of stem/osteoprogenitor cells already present in the damaged tissue would potentially be an ideal solution if the biologic limitations of these cells and their regulation could be reduced or eliminated. To this end, much research has been focused on identifying and capitalizing on the various signaling mechanisms present in bone, and on the cells necessary to carry out regeneration.

Stem/progenitor cells and differentiation in bone

The osteogenic/chondrogenic cell lineage depends on a number of signaling mechanisms to induce differentiation from a multipotent mesenchymal stem cell into a mature osteoblast/cyte or chondroblast/cyte. Mesenchymal progenitor cells committed to this lineage are characterized early on by the expression of the transcription factor Sox9. Following induction of expression of Runx2 and Osx transcription factors, these cells further differentiate into mature osteoblasts. In the absence of Osx expression, they will commit to the chondrocyte lineage (Long, 2012).

Identification of mesenchymal progenitor cells present in tissue which have not committed to a particular cell lineage has been a challenge, and localization of stem/progenitor cells in-vivo has proven elusive. Possible markers include CD166, CD73, CD44 and CD105 (Shenaq, 2015). However, these markers can also be expressed on fibroblasts (Luzzani, 2015). These markers overlap the known in-vitro mesenchymal stromal cell markers - CD 29, CD 73, CD90, CD 106, CD 166, CD 146 and Stro-I. Other candidate markers are the known embryonic stem cell markers - SSEA4, Oct4, Sox2, Nanog, Tra2-49, Tra2-54, Nestin and HLA-ABC (Marynka-Kalmani, 2010). The problem with each of these markers is that they are not entirely unique to stem cells and, therefore, cannot be used individually to locate these cells definitively in tissue samples.

Once formed, osteo/chondroprogenitor cells have several fates which can be influenced by the local environment. Osteoprogenitor cells may differentiate into mature osteoblasts, secreting osteoid (that mineralizes into woven bone) and coordinating osteoclastic remodeling activity through secretion of nuclear factor kappa-B (NF- κ B). They may differentiate into quiescent bone lining cells, which have the potential to revert back to active osteoblasts if needed. Additionally, they may differentiate into osteocytes, trapped within a bony matrix, coordinating bone remodeling via mechanical stress signaling mechanisms. Chondroprogenitor cells may follow similar analogous pathways leading to active chondroblasts or semi-latent chondrocytes. The cellular population of mineralized tissues depends on the tissue development and structure.

BONE DEVELOPMENT AND HEALING

Bone Structure: Cortical and Trabecular Bone

There are three general bone morphologies, characterized by their three-dimensional structure, cellular landscape and degree of mineralization. Cortical bone is the most highly mineralized, and therefore strongest, form present in mature bone. It is characterized microscopically by the presence of dense, circumferential structures termed “osteons” which surround a central vascular channel, the Haversian Canal. The principle cell type within these osteons are terminally differentiated osteocytes, which reside in lacunae and help coordinate bone remodeling via intercellular connections and mechanical sensing. Superficially, cortical bone is lined by a covering layer of cells and associated connective tissue referred to as the “periosteum”. Grossly speaking, cortical bone lines the superficial surface of a bony organ, providing structural integrity and protection as well as defining the overall shape.

Trabecular bone is the most common form found in adult organisms. It occupies the internal spaces and contains bone marrow - the soft, vascular tissue housing most of the cellular and fluid components of bone. It is characterized microscopically by saucer shaped “lamellae”, which are arranged either exactly parallel or perpendicular to one another. Grossly speaking, the bone is comprised of many interweaving trabeculae - peninsular type structures which contain the mineralized portion of trabecular bone and are lined by a distinct layer of cells termed the “endosteum”. Trabeculae containing red marrow

house the organism's hematopoietic stem cells. These give rise to the erythrocytes, leukocytes and other important immune-mediated cell types, including macrophages. Other trabeculae can contain white marrow, often dominated by fat tissue, but also containing non-hematopoietic connective tissue.

The third general form of bone found in the adult organism is woven bone, a less mineralized and transitional form common during development and repair. Woven bone is typically resorbed and replaced by mature bone containing both cortical and trabecular components through a coordinated action of osteoblasts and osteoclasts during remodeling (Gartner, 2007).

Formation

Two methods of natural bone development have been described extensively in the literature: endochondral and intramembranous ossification. Endochondral ossification involves the establishment of a cartilage model approximating the size and shape of the developing bone. This cartilage model is later resorbed, ossified and replaced by more dense bone tissue (Mackie, 2011). Examples of endochondral ossification include the femur and spinal vertebrae. In contrast, intramembranous bone forms directly within an osteoid matrix produced by osteoblasts, and is not preceded by a cartilage model (Berendsen, 2015). Examples of intramembranous bones include the mandible and clavicles. Eventually, the outer surfaces of all types of bone are covered by a periosteal cell layer, providing protection, vasculature and a source of stem/osteoprogenitor cells. Similarly, internal surfaces become covered with an endosteal bone-lining layer.

Bone Eminences

Muscle tendons can usually be found inserted into elevated portions of the bone surface termed “bone eminences”. Although the development of these eminences is not well-understood, recent publications have shown that cells in this area are descendants of progenitor cells distinct from those forming the bulk of the bone. Progenitor cells in eminences express Sox9 and Scx during development (Blitz, 2013; Zelzer, 2014). It is possible that cells within this region can be induced to proliferate and differentiate into active osteoblasts, providing a recruitment target for induction of bone healing.

Rat Calvarial Defects

The bones of the skull, including the calvaria, form by intramembranous ossification. The parietal ridge of the rat calvarium forms as the attachment site for the temporalis muscle, which inserts into the parietal bone (Wingerd, 1988). The ridge bone is covered by a superficial periosteum and has several different tissue types in the vicinity, each of which may harbor latent stem/progenitor cells. Thus, potential local sources of these cells include the periosteum, adipose tissue, muscle ligament, and trabecular endosteal bone lining cells that can access the bone surface through vascular trabecular openings.

Palaez et al tested the effects of varying concentrations of recombinant human BMP-2 (rhBMP-2) on bone formation in this critical calvarial defect model. They found that rhBMP-2 combined with an acellular sponge accelerated local

bone formation (Palaez, 2014). The response was dose-dependent and reached a threshold above which higher concentrations of rhBMP-2 did not produce higher rates of bone formation. However, the sources of cells mediating this rhBMP-2 mediated bone formation have not been characterized in detail.

Mechanisms of Bone Healing

The stem/progenitor cells resident within the periosteum (or endosteum) normally lay dormant unless called upon by molecular signals to proliferate and differentiate. These cells typically exhibit a flattened morphology indicative of quiescence (Miller, 1987). Once activated, these cells are seen to enlarge and convert to a cuboidal morphology indicative of high anabolic activity (Liu, 1997). Bone morphogenetic protein-2 (BMP-2) is a very well-studied and potent signaling molecule known to induce differentiation of these stem/osteoprogenitor cells.

It is known that injuries to the tibial periosteum stimulate healing of the underlying bone by endochondral ossification, whereas injuries to bone marrow heal *via* intramembranous ossification (Colnot, 2009). Based on initial studies (O'Bryhim, Jusino, DeCardona, Cote, Capetillo Theses), during healing of a critical-sized calvarial defect in the presence of rhBMP-2, the differentiated cells adjacent to the rat dura begin to lay down new bone around transient cartilaginous nuclei. In contrast, bone created near the parietal ridge shows no histological evidence of a cartilage model, regardless of the presence or absence of rhBMP-2. This offers a clue to the origin of stem/progenitor cells within a

population of cells observed proliferating near the parietal ridge shortly after surgery.

HYPOXIA AND STEM CELL ACTIVATION

During tissue injury, many environmental factors signal the body to induce an inflammatory healing response. Cytokines released by cellular players, molecular components of innate immunity such as complement, and local chemical factors such as pH and oxygen levels all play major roles in mounting a healing response. Hypoxia, which results from initial vascular damage, seems to be linked directly to stem cell activation. Reduced levels of oxygen, characteristic of areas of tissue damage, necrosis or neoplasm stimulate both angiogenesis and mesenchymal stem cell proliferation (Burke, 2013; Stiers, 2016).

Decreased oxygen level leads to higher cellular levels of the transcription factors hypoxia inducible factor 1 (HIF-1) and hypoxia inducible factor 2 (HIF-2). Each transcription factor consists of a constitutively expressed beta subunit, and a hypoxia-regulated alpha subunit. Under normoxic conditions, HIF-1 and -2 alpha are also constitutively expressed, but are rapidly ubiquitinated and subsequently degraded by the proteasome. Under hypoxic conditions, these proteins are no longer ubiquitinated; degradation no longer occurs, leading to the dimerization of the alpha and beta subunits into an active transcription factor, which binds to regulatory regions of genes coding for proteins involved in healing (Huang, 1996; Kallio, 1997). HIF-1 has angiogenic and proliferative activity (Keith, 2007). HIF-1 upregulates production of vascular endothelial growth factor

(VEGF) and stromal derived factor-1 (SDF-1), which is a potent mesenchymal stem cell recruitment signal (Das, 2010). Salim et al. investigated the effect of hypoxia on differentiation potential. They found no difference between 21% pO₂ and 2% pO₂. However, they did observe diminished osteoblastic differentiation at 0.02% pO₂ (Salim, 2004). The effects of hypoxia on bone formation remain to be fully defined.

Macrophages

Macrophages are important cellular components of both the innate/adaptive immune response, but also play a key role in the healing of hard and soft tissue. These cells begin as pluripotent hematopoietic stem cells in bone marrow that differentiate into circulating monocytes. These monocytes undergo diapedesis (crossing the vascular lining) when induced by inflammatory cytokines present in damaged, inflamed, infected or hypoxic tissue. These cells typically migrate to the area of insult 48-96 hours after a precipitating event (Eming, 2007).

Macrophages play an important role in the degradation of injured tissue that is necessary to allow for repair/regeneration. Macrophages are known to exist in two main forms: the M1 and M2 phenotype. The polarization of macrophages towards one of these phenotypes is regulated by the local environment in which they are activated. The M1 phenotype promotes an immune response through secretion of pro-inflammatory cytokines. The M2

phenotype of macrophages is involved in wound healing and is capable of secreting various cytokines important in stem/progenitor cell proliferation (Galli, 2012). Resorption of damaged bone tissue is necessary to pave the way for new bone formation. If bone resorption fails to occur at the site of injury, regeneration is not possible (Chambers, 1984). Krüppel-like factor 4 (Klf4) is a key regulatory cytokine involved in M2 macrophage polarization and is a useful immunohistochemical marker used to identify the presence of this phenotype in tissue samples (Liao, 2011). Macrophage activity in the parietal ridge region of the rat calvarium may therefore reveal important information regarding the signaling mechanisms involved in mobilizing stem/progenitor cells.

IMMUNOHISTOCHEMISTRY

Antibodies provide powerful tools for the phenotypic analysis of cell populations. The techniques of immunohistochemistry are rooted in the work of the American physician Albert Coons who first published on the technique in the 1940's (Coons, 1941). This field of light microscopy takes advantage of the highly specific relationship that exists between antibodies and their complementary antigens. Antibodies are developed to be detectable visually and can be combined with a histological specimen in a variety of ways to establish a bond with the associated antigens thought to be present in a sample. Once bound, excess antibodies can be washed off the specimen leaving behind only those that are specifically bound to the tissue. The presence of the antigens of interest,

now confirmed in the tissue by subsequent visual detection methods, can be easily studied (Dabbs, 4th edition).

Amplification of a bound antibody signal is often necessary to achieve a detectable result. This is accomplished through a mechanism of secondary antibodies and other chemical agents. Initial binding of the primary antibody produces a 1:1 association to the complementary epitope region on the antigen; however, a polyclonal primary antibody may contain immunoglobulins targeting several different epitopes on the same antigen molecule, providing the first amplification step. Subsequently, so-called secondary antibodies can be used that target different epitopes on the primary antibody. This allows for many individual secondary antibodies to bind to a single primary, providing the second level of amplification. Secondary antibodies can be covalently bonded to a fluorochrome, allowing their localization to be detected by fluorescence microscopy (immunofluorescence, IF), or they can be bonded to another compound such as biotin. Biotin can then be detected using a biotin-binding protein such as streptavidin covalently linked to an enzyme, such as horseradish peroxidase. These catalysts can then be used to form pigmented compounds that precipitate at the site of the target antigen, providing further amplification and allowing for visual observation by light microscopy. This is the basis for immunohistochemistry (IHC).

Typically, the primary antibody has been developed in a species such as rabbit or goat, different from the species the antigen originated from, and usually

different from the species under examination in a study. Although techniques have been developed to allow primary antibodies to be used to detect antigens in the same species, they are more challenging and prone to background issues. Similarly, the secondary antibody must be developed in a third species (e.g. horse, goat) different from either the tissue sample under study or the primary antibody. In order to reduce unwanted, non-specific binding of the primary and secondary antibodies to the tissue sample, a blocking step is utilized in which serum or pre-immune immunoglobulins, often from the third species, are added to the tissue sample. The goal is to occupy and mask the majority of low affinity, non-specific binding sites within the tissue, leaving only sites for the primary antibody to bind specifically to its target antigen, or the secondary antibody to bind to the primary. Other blocking steps (e.g., inhibition of endogenous peroxidase activity) may be required, depending on the detection systems employed.

IMMUNOFLUORESCENCE

Immunofluorescence (IF) is a subcategory of immunohistochemistry that involves fluorochrome components that fluoresce at specific wavelengths when illuminated with certain light wavelengths. Fluorochromes can either be attached directly to the primary antibody, or to the secondary polyclonal antibodies, thereby providing amplification. The latter technique is known as indirect or secondary immunofluorescence (Fritschy, 2001). Indirect immunofluorescence has the additional logistical benefit of utilizing more common, unmodified (and typically less expensive) primary antibodies to target the antigens of interest with

one fluorescent secondary antibody that can recognize primary antibodies from the same species. Importantly, two or more different fluorochromes (usually in conjunction with antibodies from different species), can be analyzed on the same section, allowing for colocalization of expression within the same cell (frequently using confocal microscopy). A further benefit of IF is the ability to use digital quantification of a signal and software to analyze the strength and distribution of a signal in a tissue sample.

Available Candidate Stem Cell Markers

Mesenchymal stem cell markers include CD73, CD90, CD105, CD166, CD172alpha, and CD271. Pluripotent stem cell markers include Tra-1-60, CD133, and CD309 (Luzzani, 2015). Additional markers of interest include Musashi, Sox2 and Klf4, the latter also serving as a marker for the M2 macrophage phenotype. Since stem cells must proliferate when induced, proliferating cell nuclear antigen (PCNA) serves as a useful tool to quantify proliferation.

SUMMARY

In the rat calvarial defect model, bone regeneration has been observed to occur in a dose-dependent relationship to rhBMP-2. In the area near the dural lining, this appears to involve islands of cartilage as a precursor step. However, in the parietal ridge region, bone regeneration has been observed to occur with no cartilage precursors, i.e., intramembranous ossification. Additionally, this ridge-derived osteoid formation appears to occur at least somewhat independent

of the concentration of rhBMP2 used, suggesting a different cell lineage is present.

PURPOSE

The purpose of this study is twofold: to provide an initial characterization of proliferative osteogenic stem/progenitor stem cells present in the parietal ridge, and to investigate the temporospatial relationship between these proliferative cells and two candidate signaling mechanisms for their activation, hypoxia and M2 polarized macrophages. The rat critical-sized calvarial defect model, and previously prepared histological samples, will be utilized. Phenotypic marker expression will be evaluated using immunohistochemistry and immunofluorescence. Cell proliferation will be quantified using PCNA expression. Stem/progenitor cells will be identified using a panel of candidate markers such as Sox2, Klf4 and Musashi-1, and osteogenic cells by expression of Runx2, Osx and other more downstream genes. Chondrocyte lineage markers such as Sox9 will also be evaluated. The distribution of HIF-1 and SDF1 expression and the distribution of M2 macrophages relative to parietal ridge bone formation will be also examined.

HYPOTHESES

HYPOTHESIS #1

There exists a population of stem/progenitor cells in the parietal ridge region of the rat calvarium that may be induced by injury to proliferate and differentiate into the osteoblast, but not chondrocyte lineage, regardless of rhBMP-2 treatment.

HYPOTHESIS #2

Stem/progenitor cells will show upregulated expression of HIF-1 and downstream targets such as SDF-1 following surgical creation of the critical-sized bone defect.

HYPOTHESIS #3

M2 Macrophages will be present in the area of bone formation and will express pro-regenerative proteins.

SPECIFIC AIMS

AIM #1

Determine cellular co-localization of markers for proliferation and stem/progenitor cells in the parietal ridge region of the rat calvarium during a two week period following surgical creation of a defect in the presence of different amounts of rhBMP-2. IHC and IF will be used with a set of antibodies targeting candidate stem cell markers, as well as osteo- and chondroprogenitors. Where appropriate, the proportion of cells expressing a given marker (such as PCNA for proliferation) will be quantified. Results from these experiments will provide a characterization of the cell populations present in the parietal ridge region associated with bone formation, and their response to rhBMP-2.

AIM #2

Quantify cellular upregulation of HIF-1 and downstream markers such as SDF-1 in the parietal region of the rat calvarium during healing of the critical-sized bone defect. IHC and IF will be used with a set of antibodies targeting HIF-1 and other proteins to determine the presence of their signals within the calvarial tissues. The proportion of signal expressed within the various tissues will be quantified. Results from these experiments will provide circumstantial evidence for the extent to which hypoxia is involved in bone regeneration in the rat calvarium.

AIM #3

Identify and quantify the presence of M2 macrophages in the parietal ridge region of the rat calvarium. IHC and IF will be used with a set of antibodies to include CD68 and Klf4. The amount of cells present will be quantified and their temporospatial relationship to the defect will be analyzed. These experiments will indicate the presence of macrophages within the healing defect and deduce the extent of their polarization.

MATERIALS AND METHODS

OVERVIEW

The goals of this study are to identify the phenotype of proliferating cells in the parietal ridge region of the rat calvarium during healing, and to assess the effect that hypoxia has on recruitment of stem/progenitor cells. Previous studies carried out at by residents from Tingay Dental Clinic examined the effect of rhBMP-2 in an absorbable collagen sponge (ACS) on bone regeneration utilizing one hundred and fifty Sprague-Dawley rats (Jusino, O'Bryhim, DeCardona). These animals (age 11-13 weeks, weight 250-300g) were divided into three treatment groups: 20 µg/site (rhBMP-2/ACS), 5 µg/site (rhBMP-2/ACS), and ACS alone (carrier control = 0 µg/ml dilution buffer).

SURGICAL PROCEDURE AND MATERIALS

All aspects and procedures of animal management were approved by the Institutional Animal Care and Use Committee, Dwight David Eisenhower Army Medical Center, Fort Gordon, GA. A through-and-through, critical-size, 8 mm-diameter, calvarial osteotomy defect was created using a trephine diamond bur supplemented with sterile saline irrigation. After creation of the calvarial defect, ACS containing one of two different concentrations of rhBMP-2 or buffer alone with no rhBMP-2 was placed into the wound space. The graft material was covered with a 10 mm-diameter titanium mesh to provide wound stability and to prevent epithelial migration into the defect space. Primary closure was obtained

using surgical clips. Sample animals at each dosage concentration were euthanized on either Day 1, 3, 5, 7 or 14, the heads collected, and fixed in 10% buffered formalin solution. The calvarial region containing the defect was sectioned coronally with a Buhler saw and divided into posterior and anterior halves. The anterior half was processed for paraffin embedding and sectioning. (The posterior half was preserved in ethanol for future studies.)

CURRENT STUDY

These samples will be further examined using immunohistochemical and immunofluorescence techniques to determine the presence and distribution of relevant markers for stem/osteoprogenitor cells and M2-polarized macrophages. Additionally, the presence and extent of signaling components of hypoxia regulated pathways will be evaluated. The overall design of this study is illustrated in Figure 1.

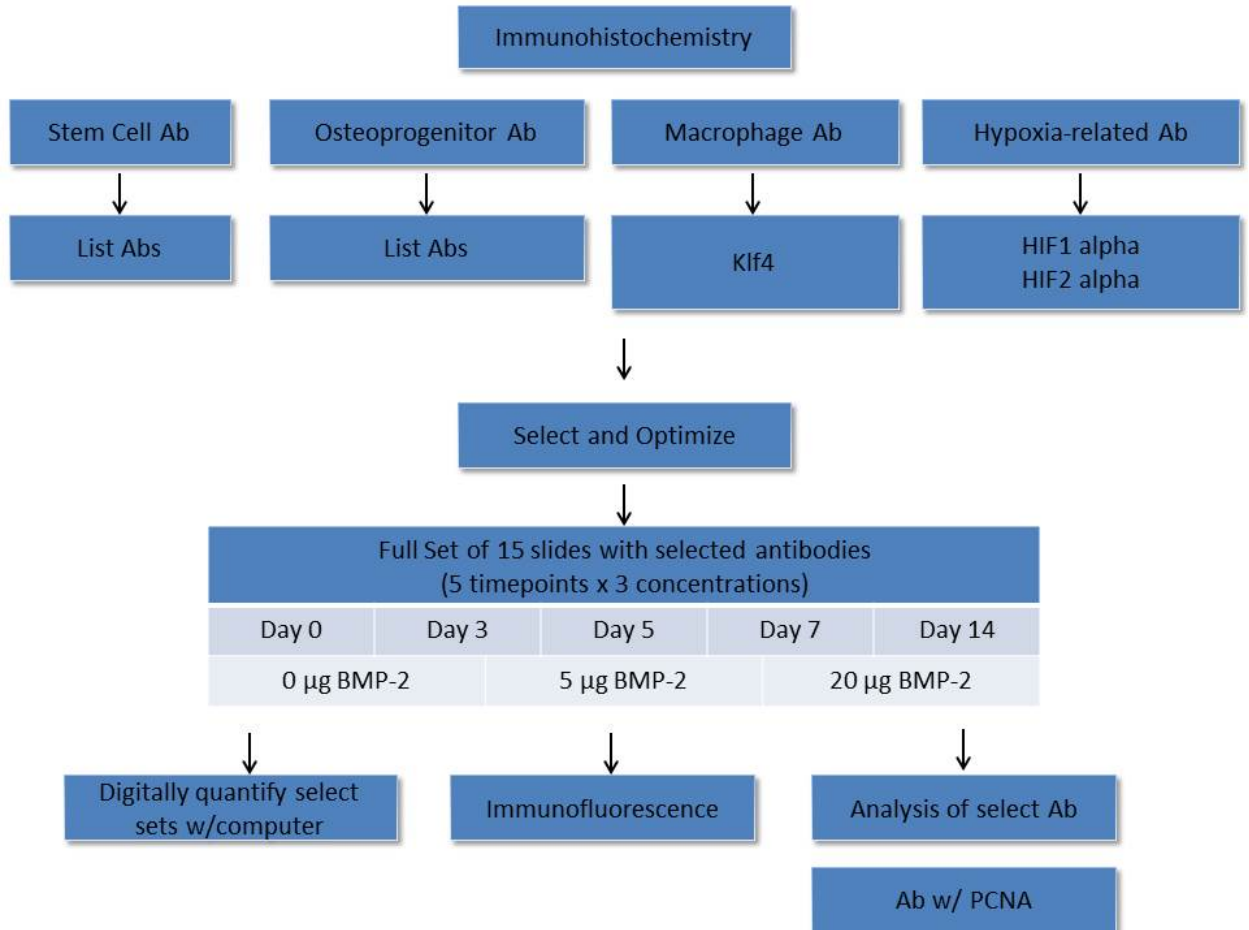


Figure 1: Immunohistochemistry will be performed using antibodies known to be expressed in stem/osteoprogenitor cells, macrophages and components of the hypoxia signaling pathway. Pilot experiments will be used to determine if an antigen is present, then the antibody concentration will be optimized and applied to a complete set of 15 slides: 5 timepoints (0, 3, 5, 7, 14 days) and three concentrations of rhBMP-2 (0µg, 5 µg, 20 µg).

DETAILED METHODOLOGY

Immunohistochemistry “Standard” Protocol

Immunohistochemistry using selected antibodies and 5µm sections processed from paraffin blocks will be performed to quantify the absolute number, proportion, and physical distribution of cells expressing a particular antigen. Antigen detection in sections will use primary antibodies (typically goat or rabbit), and appropriate species- and immunoglobulin-matched biotinylated or ALP-conjugated secondary antibodies from various commercial sources.

Slides will be heated at 60°C for 2 hours to promote tissue adherence and to melt the paraffin, and then placed in a xylene series for exhaustive deparaffinization, followed by rehydration in an ethanol series (100% x 5 min, 95% x 5 min, 95% x 5 min, 70% x 5 min), and finally in deionized water. A commercial antigen retrieval solution at 1x (Diva Decloaker, Biocare Medical, Concord, CA, USA) will be used in a carefully controlled stepwise heat treatment, with a timed step at 121°C (30 sec) in a programmable pressure chamber (Decloaking Chamber™, DC2002, Biocare Medical, Concord, CA, USA), followed by a rapid, controlled reduction in temperature and pressure. After washing in Tris-HCl buffer with 0.9% sodium chloride (TBS), non-specific antibody binding will be blocked by pre-incubating sections with 2.5% normal horse serum (NHS) or 2.5% normal goat serum (NGS) for 20 min at room temperature in a humidity chamber.

Appropriate dilutions of primary antibodies will be established empirically, starting with dilutions of 1.5, 1.0 and 0.5 µg/ml prepared in 1.25% horse serum or 1.25% goat serum. Sections will be incubated with the primary polyclonal or monoclonal antibodies overnight at 4°C in humidified chamber. Sections will then be washed in TBS buffer with 0.025% Tween-20. (TBST) and then incubated with biotinylated secondary antibodies (diluted 1:500 in TBST) for 1 h at room temperature in a humidified chamber. After washing, sections will be treated with hydrogen peroxide to block endogenous peroxidase activity, and then a commercial peroxidase-based detection system will be utilized to localize antigens. Diaminobenzidine (DAB) will be used as the chromogen to give a brown stain. Sections will then be counterstained using hematoxylin. Slides will have cover-slips placed over them using mounting medium. The presence and distribution of antigen and the staining intensity will then be evaluated by light microscopy.

Immunofluorescence Protocol

Immunofluorescence will be performed as described for immunohistochemistry with the following modifications:

1. An autofluorescence quenching step will be performed during the initial alcohol wash series. After the last 95% EtOH wash, samples will be immersed in 0.25% NH₃ in 70% EtOH for 1 hour. This will be followed by the standard 5 minute wash in 70% EtOH.

2. An additional step after the 2.5% horse serum block will be performed, utilizing Sudan black for background fluorescence quenching. Samples will be immersed in a Sudan black mix (0.2g Sudan black dissolved in 200mL of 70% EtOH filtered through doubled Whatman #2 into a clean flask) and rinsed in TBST three times for five minutes.
3. No hydrogen peroxide blocking step will be performed.
4. For secondary antibody preparation, a mixture of 13 μ L of fluorescent secondary per ml of TBST will be used. The fluorescent secondary antibody will match the species of primary.
5. For cover slipping, the PAP pen perimeter will be removed with a Q-tip dipped in xylene, and the section covered with 1-2 drops of DAPI mounting medium. After cover slipping. The sample will be allowed to sit and harden at room temperature in a dark environment overnight, then stored at -20°C .

Appropriate combinations of pairs of antibodies (and red and green fluorophore-linked secondaries) will be used to confirm co-expression, as determined from the IHC results. For example, PCNA + Sox-9, Sox-9 + Runx-2, and Runx-2 + PCNA could be used to show proliferation of osteochondroprogenitors.

RESTATEMENT OF HYPOTHESIS #1: Stem/progenitor cells

There exists a population of stem/progenitor cells in the parietal ridge region of the rat calvarium that may be induced by injury to proliferate and differentiate into the osteoblast, but not chondrocyte lineage, regardless of BMP-2 treatment.

Anticipated Results

Initial experiments will identify candidate stem cell and progenitor stem cell markers. Preliminary data indicate that Sox-2 and Runx-2 are candidates. Combinations of these markers will be evaluated for co-expression within cells. PCNA will be used as the marker for cell proliferation. Our hypothesis predicts Sox-2, Runx-2, later osteoblast differentiation (e.g. osteocalcin).

Graphical Depiction of Results

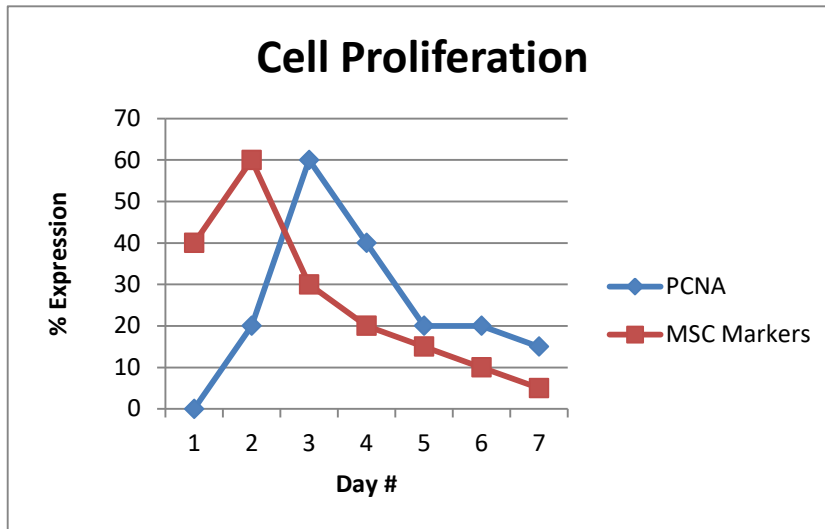


Figure 2: We expect cellular proliferation to peak at Day #3 as stem cell activation has produced significant osteoblastic/chondroblastic cells, which will begin to produce cartilage and osteoid. Mesenchymal stem cell markers should show a peak in expression around Day #1 and #2, indicating the initial differentiation.

RESTATEMENT OF THE HYPOTHESIS #2: HIF-1 and SDF-1

Stem/progenitor cells will show upregulated expression of HIF-1 and downstream targets such as SDF-1 following surgical creation of the critical-sized bone defect.

Detailed Methodology

Previously processed slides will be used to identify HIF-1 and SDF-1 expression. These slides were prepared and processed at DCI, Fort Gordon, GA in 2014-2016 (Kawaguchi, unpublished).

Anticipated Results

We expect HIF-1 expression to be high initially, representative of the hypoxic conditions created by the wound environment. This should lead to downstream expression of SDF-1 peaking a day after the peak of HIF-1 expression.

Graphical Depiction of Results

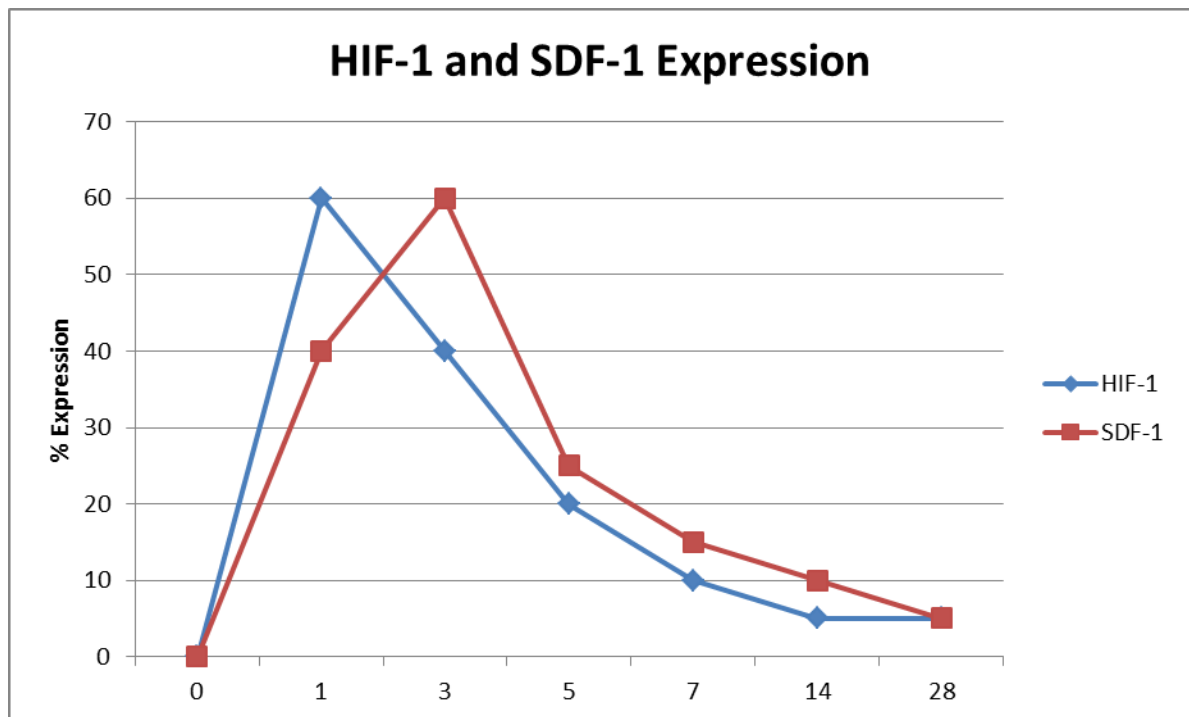


Figure 3: HIF-1 expression should show a peak at Day #1. SDF-1 peak expression should appear the following day after being activated by elevated HIF-1 levels. Both should show a gradual decline as neovascularization restores normoxic conditions.

RESTATEMENT OF THE HYPOTHESIS #3: M2 Macrophages

M2 Macrophages will be present in the area of bone formation and will express pro-regenerative proteins.

Detailed Methodology

Slides prepared as previously discussed will be stained with Klf4 and CD68 to investigate the presence of M2 polarized macrophages in the parietal ridge region.

Anticipated Results

We expect these markers to be elevated early on due to hypoxic conditions then gradually fall as vasculature is restored.

Graphical Depiction of Results

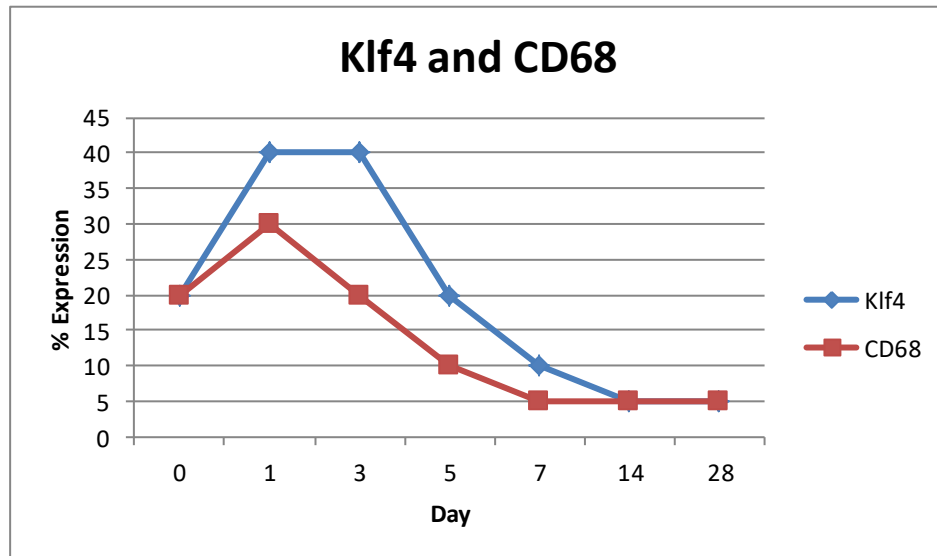


Figure 4: Both Klf4 and CD68 should peak early on as hypoxia induces polarization of local macrophages to the M2 phenotype. As normoxic conditions are restored, these markers should decline with time.

INDEPENDENT VARIABLES

Independent variables include time (continuous, treated for statistical analysis as categorical ordinal, five levels), and dose (categorical ordinal, three levels), each candidate marker is a potential variable (multiple, categorical nominal).

DEPENDENT VARIABLE

Presence or absence of marker expression (categorical nominal). Select markers will be evaluated for the percentage of positive cells and/or percentage of co-expressing cells (continuous within percentage limits).

DATA ANALYSIS

This is primarily a descriptive study to examine the patterns of gene expression in the calvarial defect bone regeneration model. Visual examination via light microscopy to confirm presence of markers will be used.

RESULTS

Krüpple-like factor 4 (KLF-4)

Day #1

At the initial time point, no significant presence of KLF-4 positive osteoblastic/cytic cells was observed in any sections regardless of rhBMP-2 concentration. Osteocytes and bone lining cells within the apex of the parietal ridge appeared homogenous throughout and displayed no characteristics distinct from those within the cavarial base. No regions of increased mitosis were evident. However, a significant presence of KLF-4 positive inflammatory cells was seen throughout the connective tissue lining the defect.

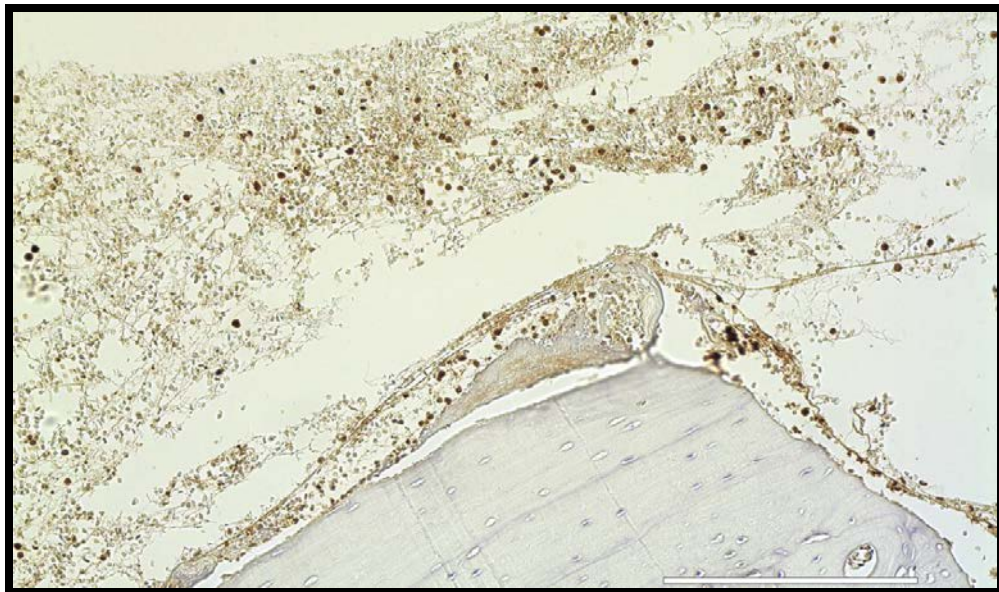


Figure 5: KLF-4 Day1 0 μ g rhBMP-2 1.10⁻⁶, 20X

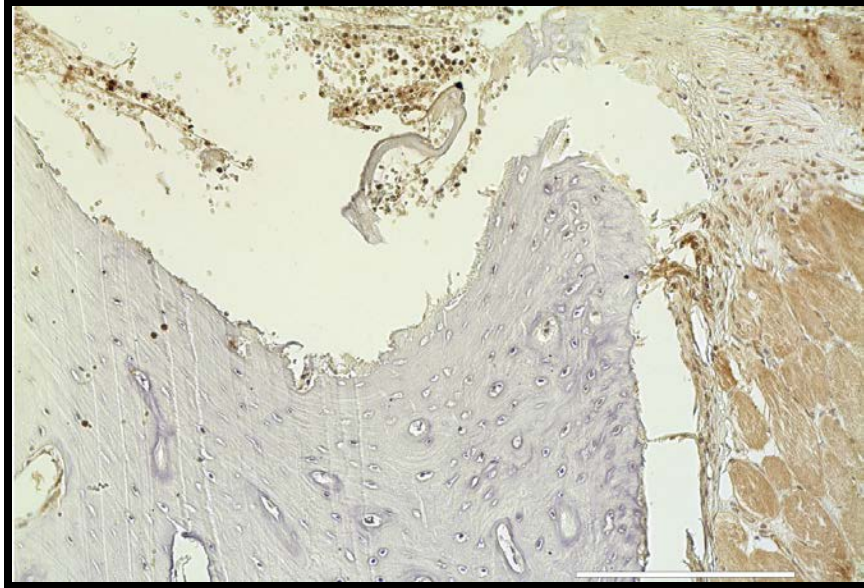


Figure 6: KLF-4 Day1 5µg rhBMP-2 1.8-15, 20x

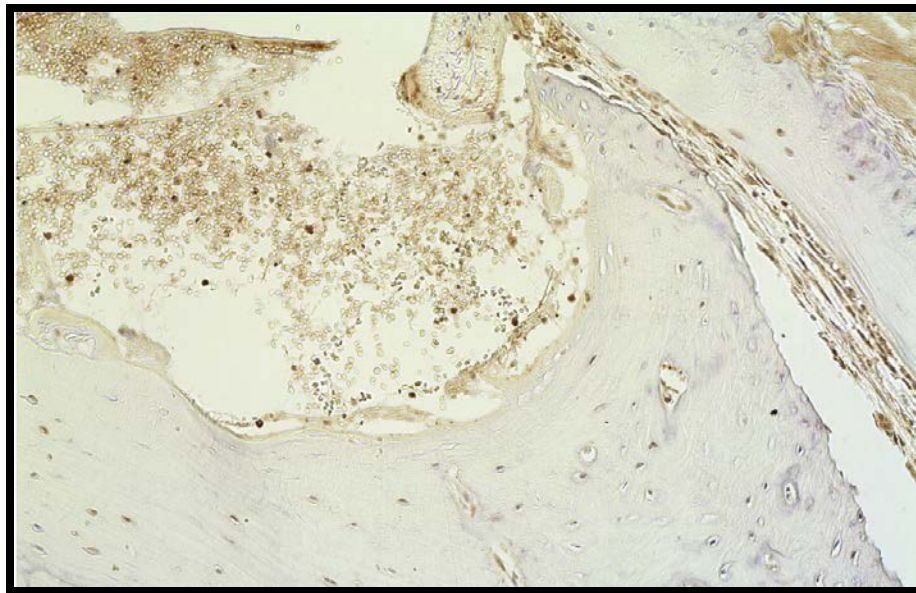


Figure 7: KLF-4 Day1 20µg rhBMP-2 1.25-14, 20x

Day #3

Cells found in the apex region of the parietal ridge were seen to begin proliferating and migrating along the slopes in a general direction toward the defect margins. This proliferation was pronounced and appeared independent of the concentration of rhBMP-2. Although the periosteum separated in some

samples due to processing, the relationship between the migrating front and bone lining cells was evident.

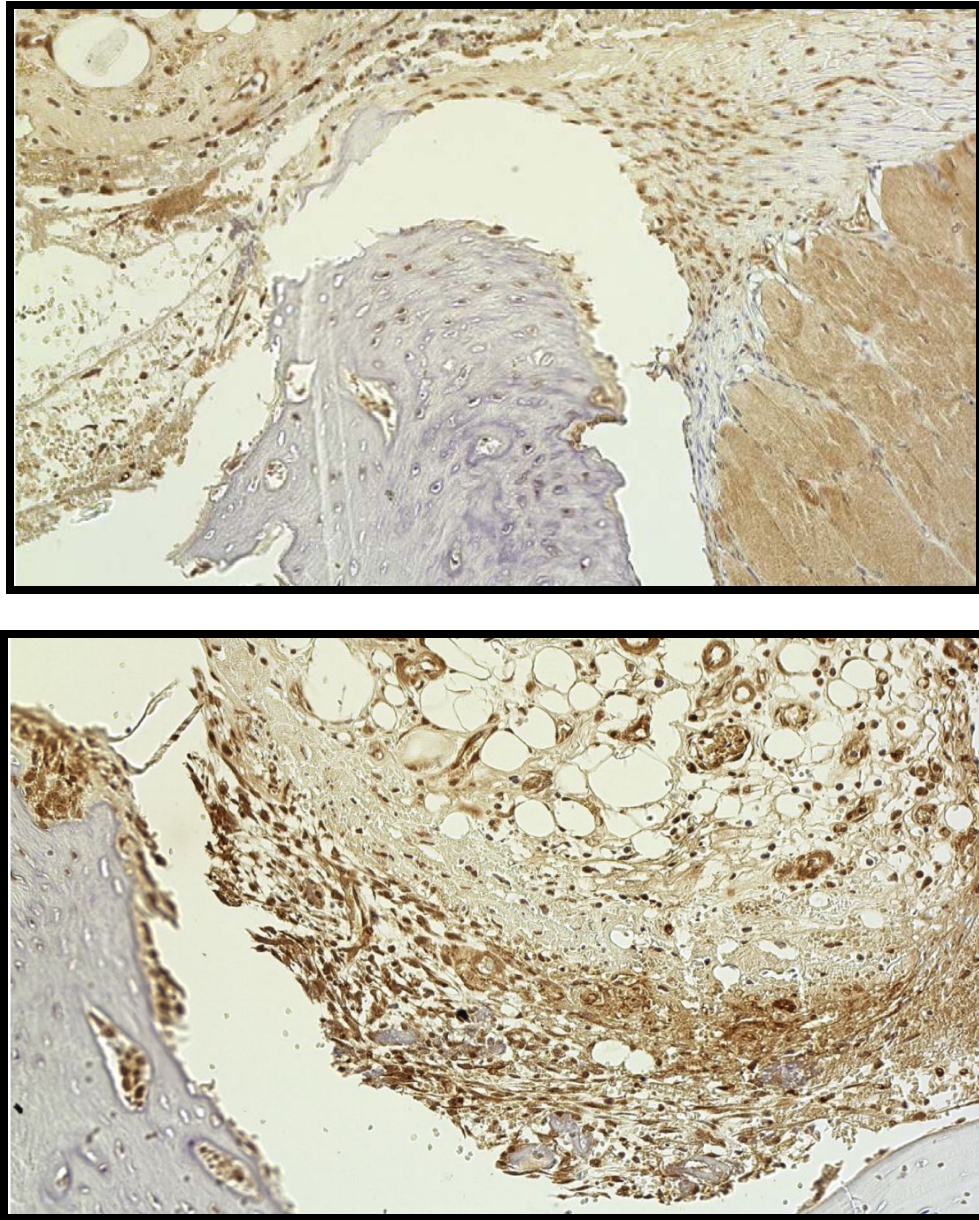


Figure 8: KLF-4 Day3 0 μ g rhBMP-2 3.37-14, 20x

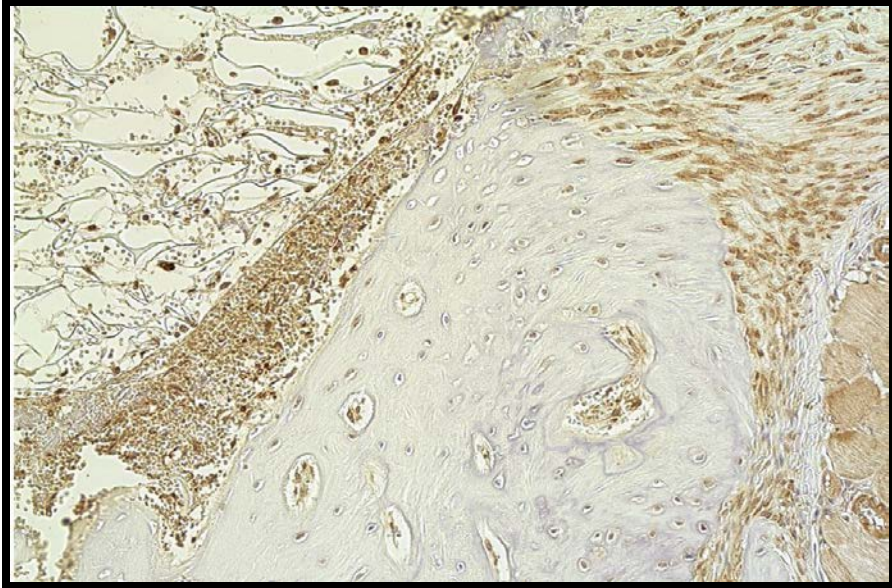


Figure 9: KLF-4 Day3 5µg rhBMP-2 3.32-9, 20x

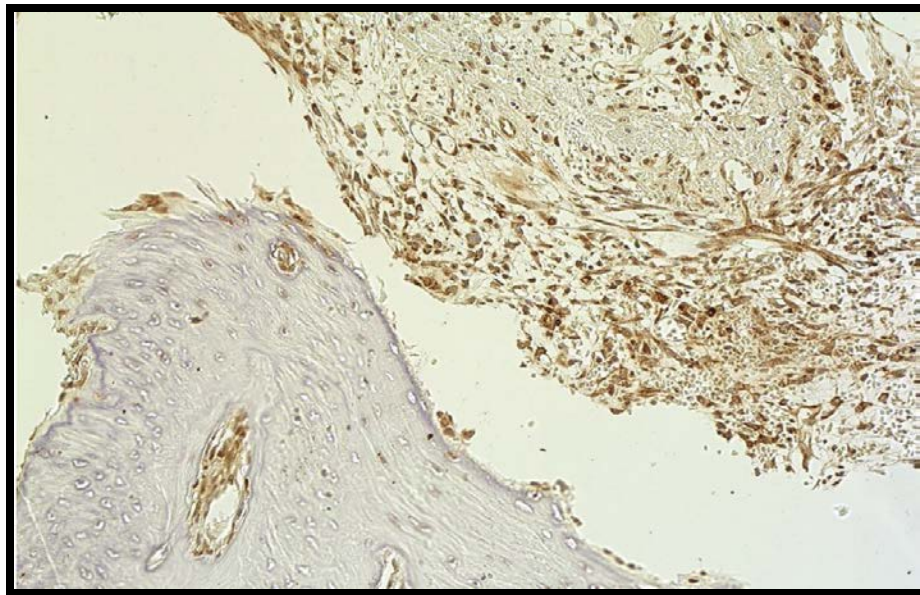


Figure 10: KLF-4 Day3 20µg rhBMP-2 3.39-9, 20x

Day #5

At the third time point, activity of regenerative cells was abundant. New connective tissue was laid down between the ridge apex and defect margin. Isolated areas of newly synthesized osteoid were observed suggesting the new proliferation of cells contained a population which was differentiating along the

osteoblastic lineage. Osteoid formation was observed at each concentration of rhBMP-2 and did not appear to positively correlate with the level of micrograms present.

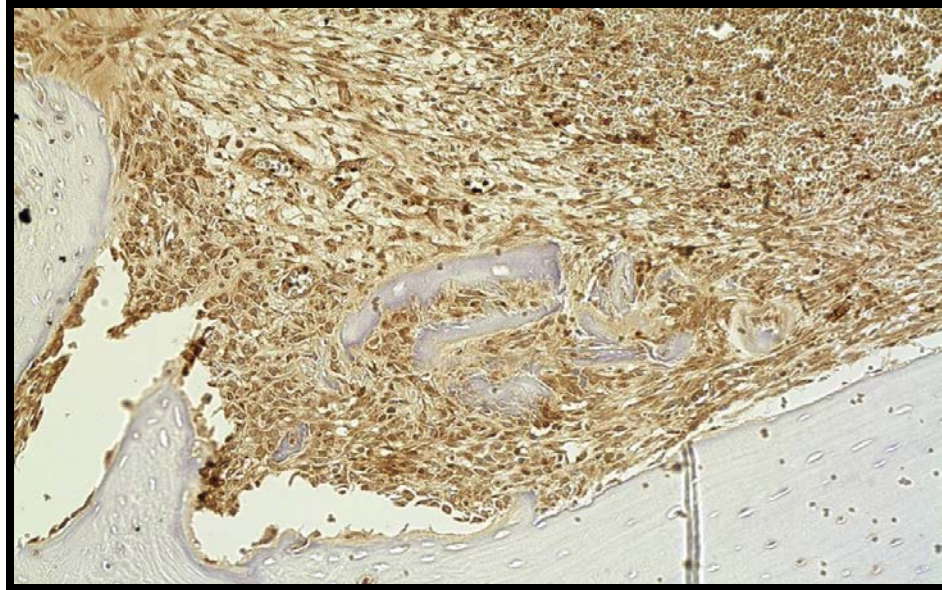


Figure 11: KLF-4 Day5 0 μ g rhBMP-2 5.103-2, 20x

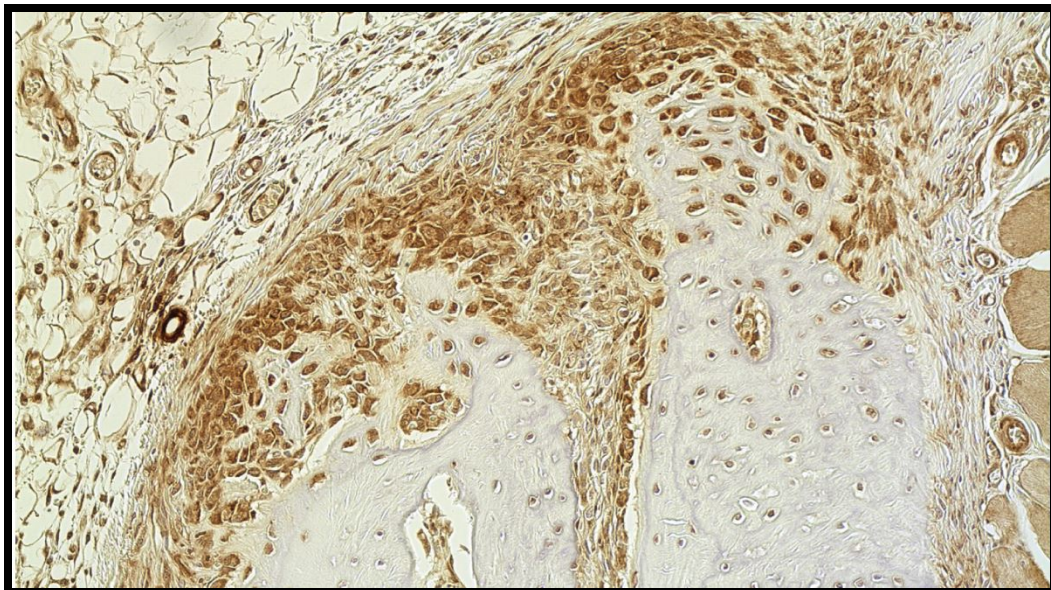


Figure 12: KLF-4 Day5 5 μ g rhBMP-2 5.95-4, 20x

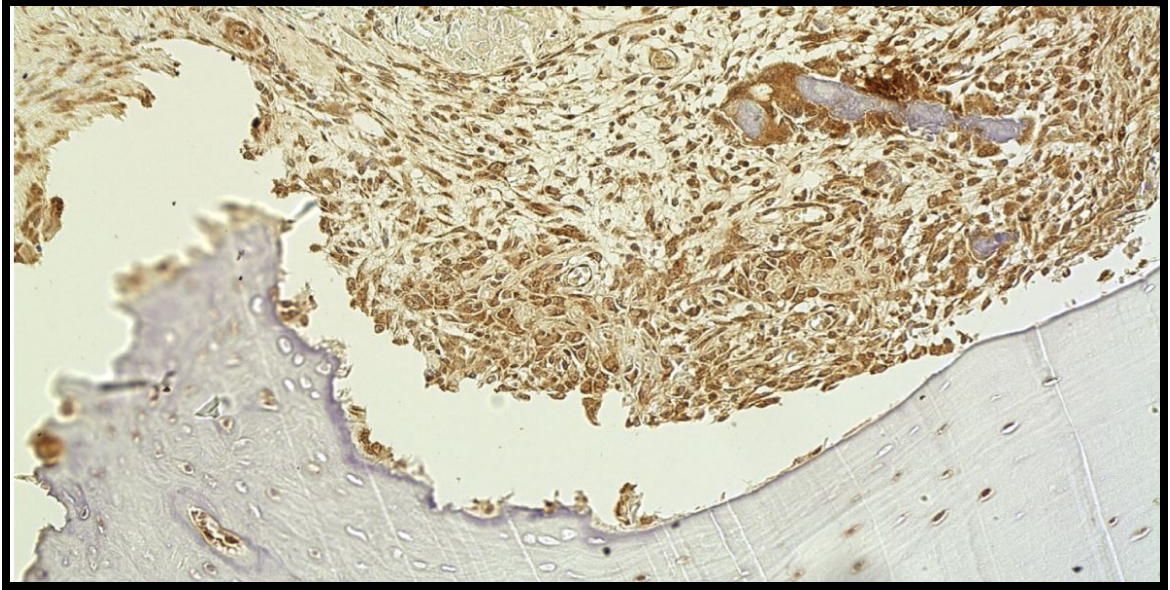


Figure 13: KLF-4 Day5 20 μ g rhBMP-2 5.90-15, 20x

Day #7

No appreciable differences were noted on day #7 with respect to osteoblast-like proliferation and bone formation. Areas of isolated osteoid continued to appear along medial slope of parietal ridge originating from the region of bone eminence cells. Cuboidal cells present along the periosteal layer seemed to be the source of much of the secretory activity.

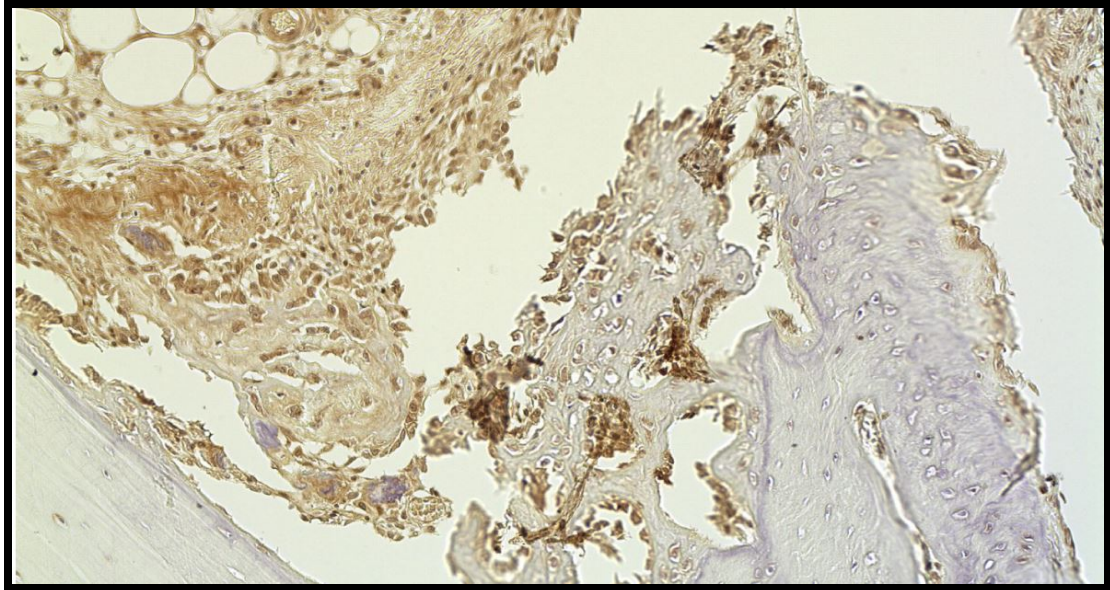


Figure 14: KLF-4 Day7 0µg rhBMP-2 7.131-7, 20x

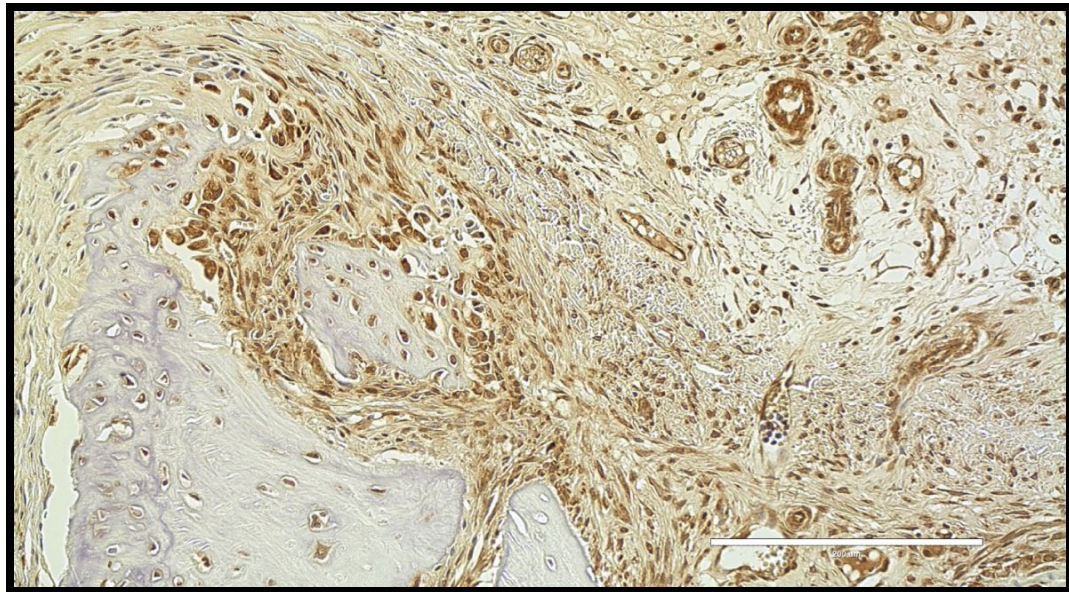


Figure 15: KLF-4 Day7 5µg rhBMP-2 7.126-15, 20x

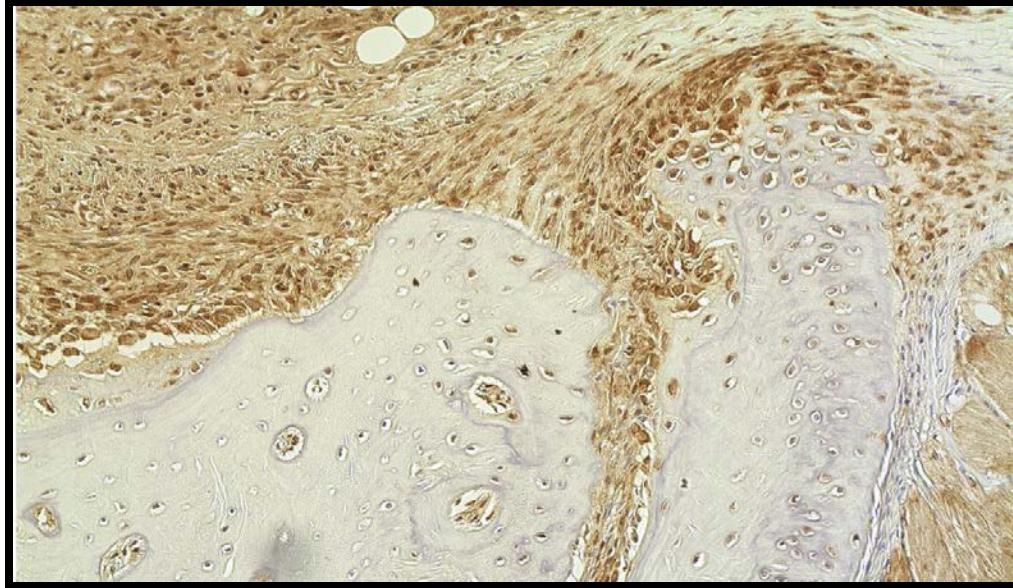


Figure 16: KLF-4 Day7 20 μ g rhBMP-2 7.127-3 20x

Day #14

By two weeks, significant new bone formation occurred. Reversal lines are clearly evident at the junction between the parietal ridge and newly-formed osseous tissue. Proliferation of the trabeculae were oriented medially in the direction of the calvarial defect. Cuboidal cells were evident along areas of new bone formation suggesting that healing was still actively occurring.

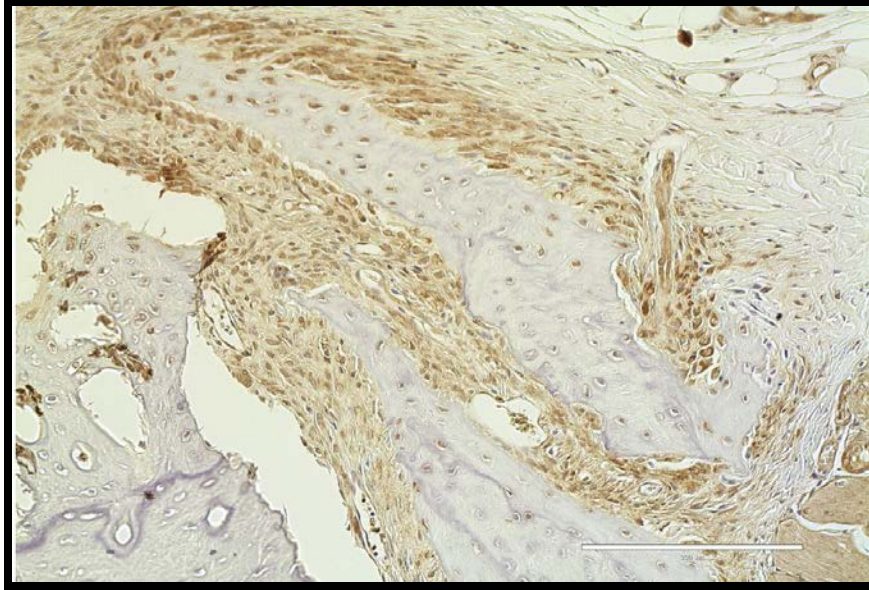


Figure 17: KLF-4 Day14 0µg rhBMP-2 14.70-4, 20x

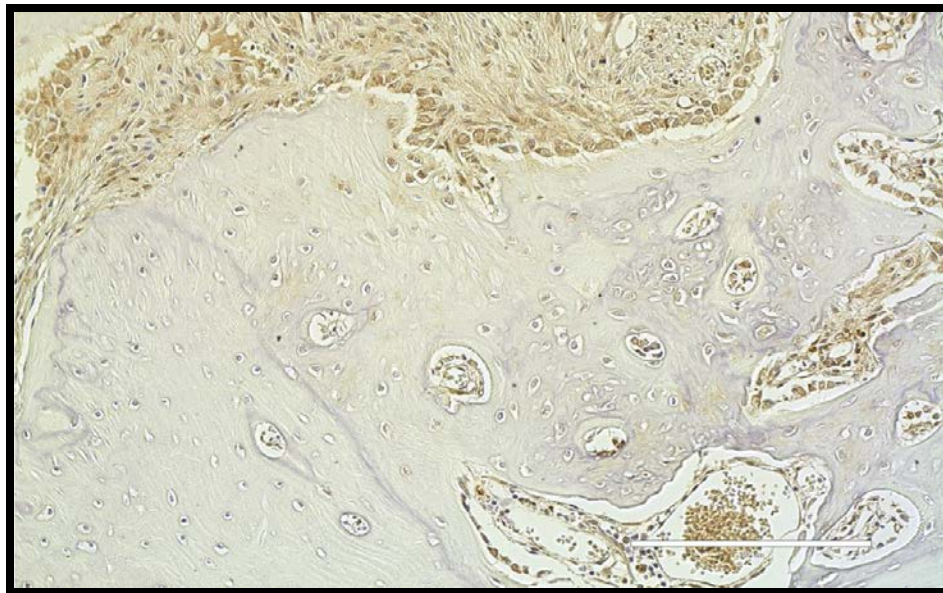


Figure 18: KLF-4 Day14 5µg rhBMP-2 14.71-13, 20x

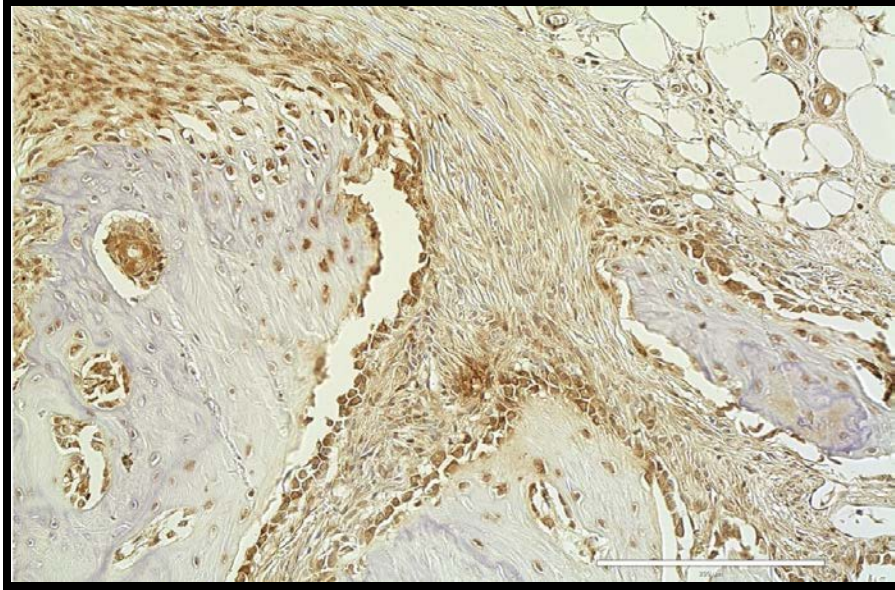


Figure 19: KLF-4 Day14 20 μ g rhBMP-2 14.63-5 20x

With the continued presence of KLF-4 positive cuboidal cells at day #14, it is likely that the proliferative lifespan of this subset of osteoblast-like cells were not fully captured in this time frame. Furthermore, the lack of an obvious difference in quantity of osteoid production in this region supports the hypothesis that this select group of osteoblastic precursors proliferates in this fashion independent of rhBMP-2 concentrations.

RNA-binding Protein Musashi Homolog 1 (Msi1)

Day #1

When compared to their counterparts within the calvarium below, osteocytes were observed to be positive for Msi1 only in the most superior regions of the parietal ridge, suggesting the presence of a subset of osteocytes (and possibly bone lining cells). Nuclei appear larger and more darkly-stained near the apex of the parietal ridge compared to nuclei in more inferior regions.

This was observed across all concentrations of rhBMP-2 with no apparent differences with respect to the size or numbers of cells exhibiting the response.

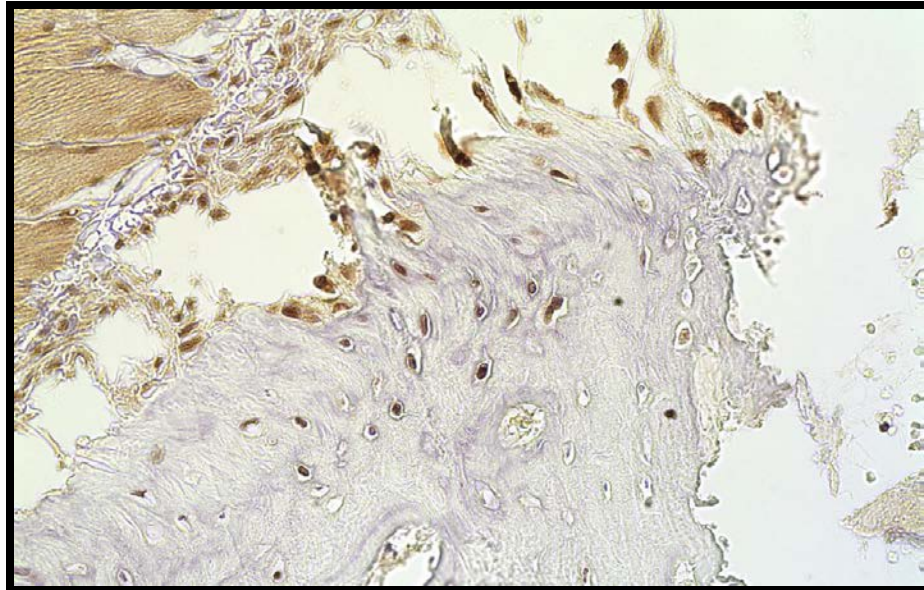


Figure 20: Msi1 Day1 0µg rhBMP-2 1.4-8, 40x

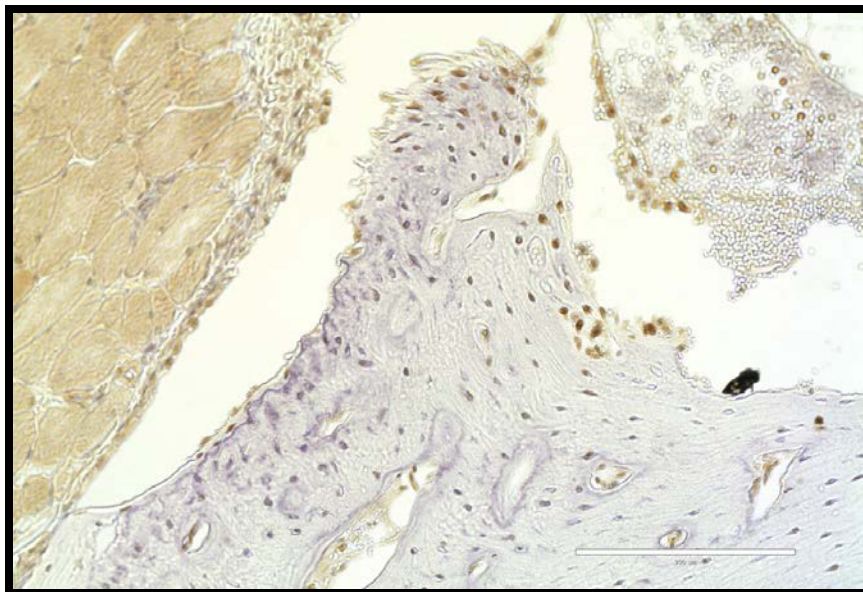


Figure 21: Msi Day1 5µg rhBMP-2 1.2-6, 20x

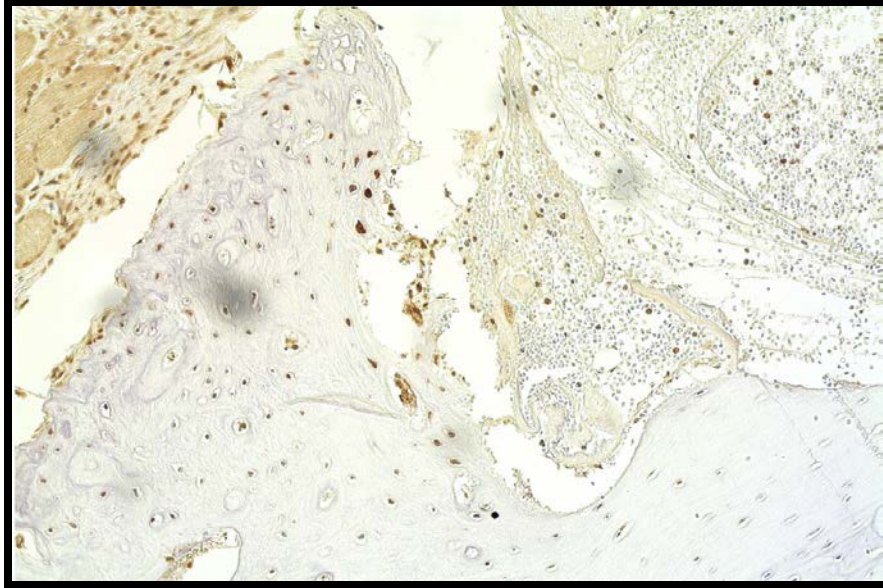


Figure 22: Msi Day1 20 μ g rhBMP-2 1.3-6, 20x

Day #3

Significant changes in the Msi1 positive osteocytes within the ridge apex were not apparent at day #3. As bone lining cells began to proliferate and lay down osteoid, the most superior osteocytes remained positive for Msi1 expression and enlarged nuclei. Fibroblast-like cells stained positive for the presence of Msi1 along the medial slope of the ridge eminence. This activity is best observed in Figure 24 at 4x magnification. Msi1 positive cells are found originating at the tendon insertion point and proliferate inferiorly and medially.

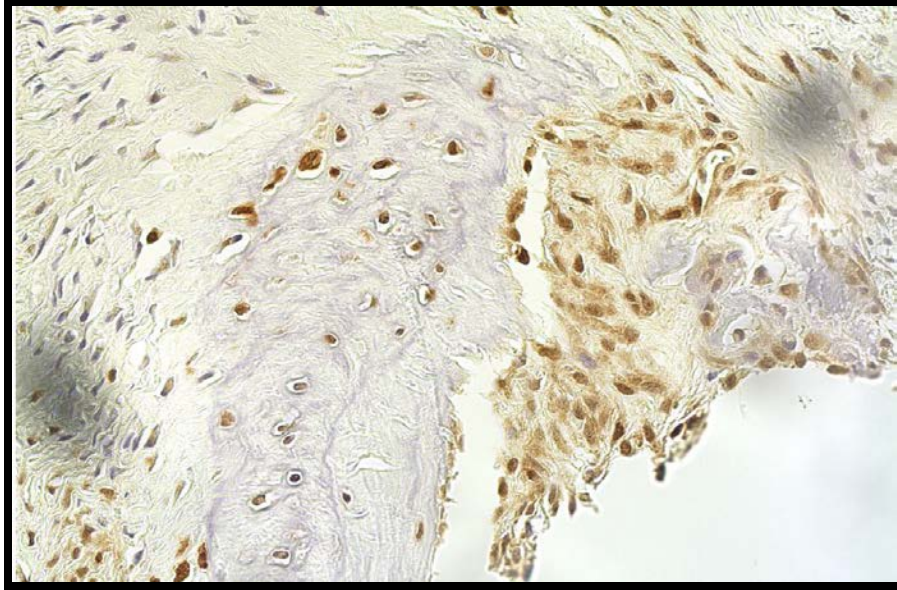


Figure 23: Msi1 Day3 0 μ g 3.28-11, 40x

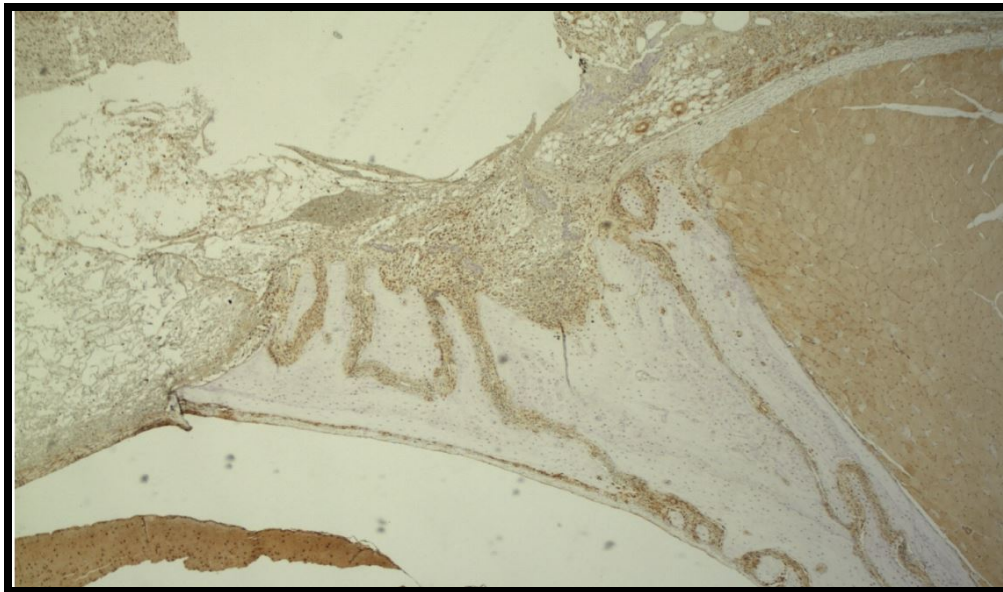


Figure 24: Msi1 Day3 5 μ g 3.29-11, 4x

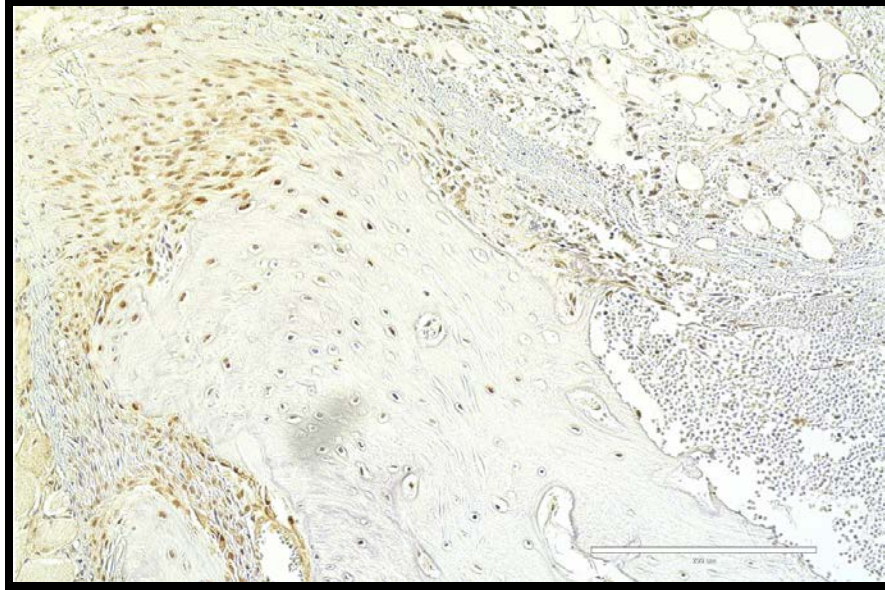


Figure 25: Msi1 Day3 20 μ g 3.33-9, 20x

Day #5

Osteoblastic proliferation remained similar to day #3. Cell activity was seen near the ridge crest but no significant differences in signal intensity or range of expression was observed. This remains consistent with the hypothesis of a distinct osteoblastic lineage, positive for Msi1 expression, unresponsive to changes in rhBMP-2 concentrations.

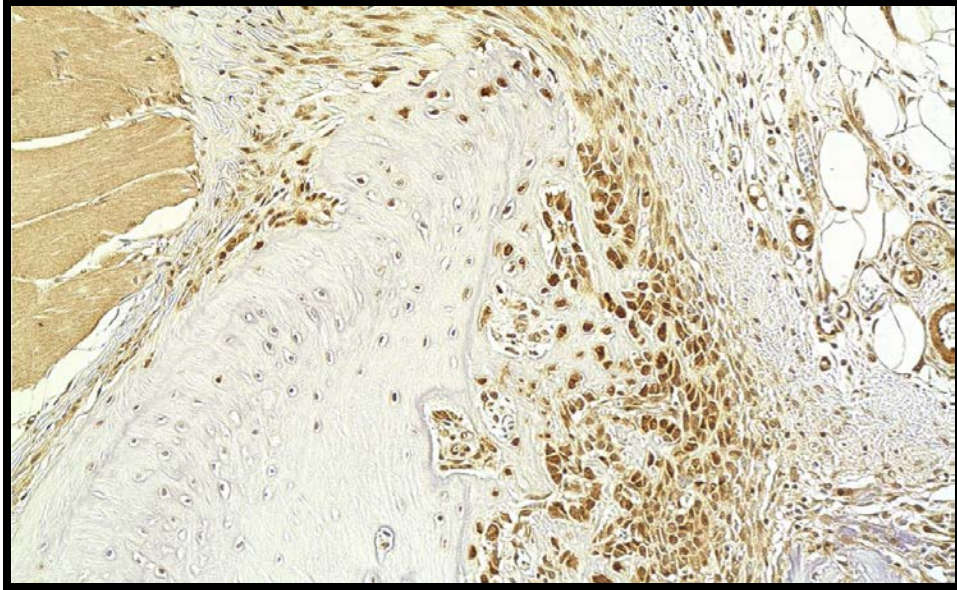


Figure 26: Msi1 Day5 0 μ g 5.82-13, 20x

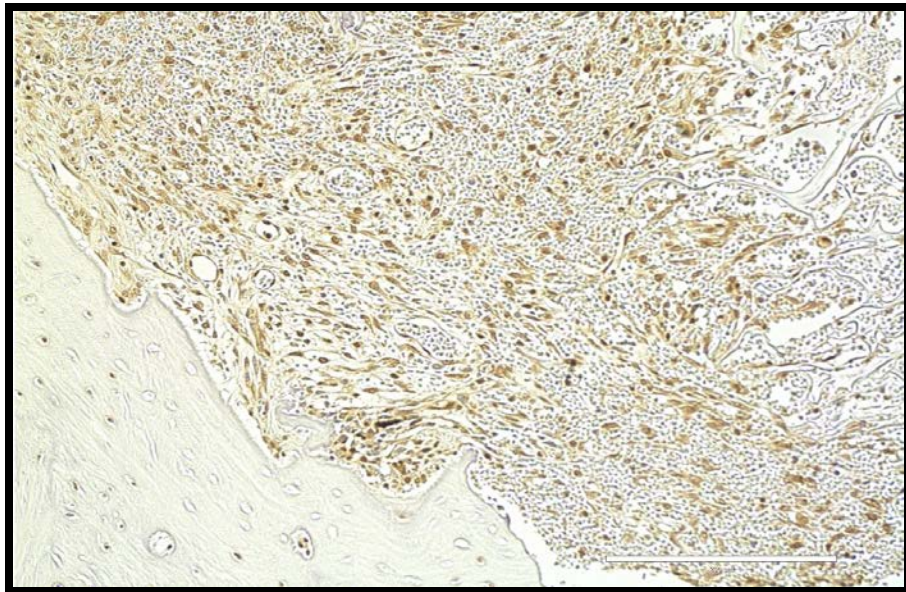


Figure 27: Msi1 Day5 5 μ g 5.104-7, 20x

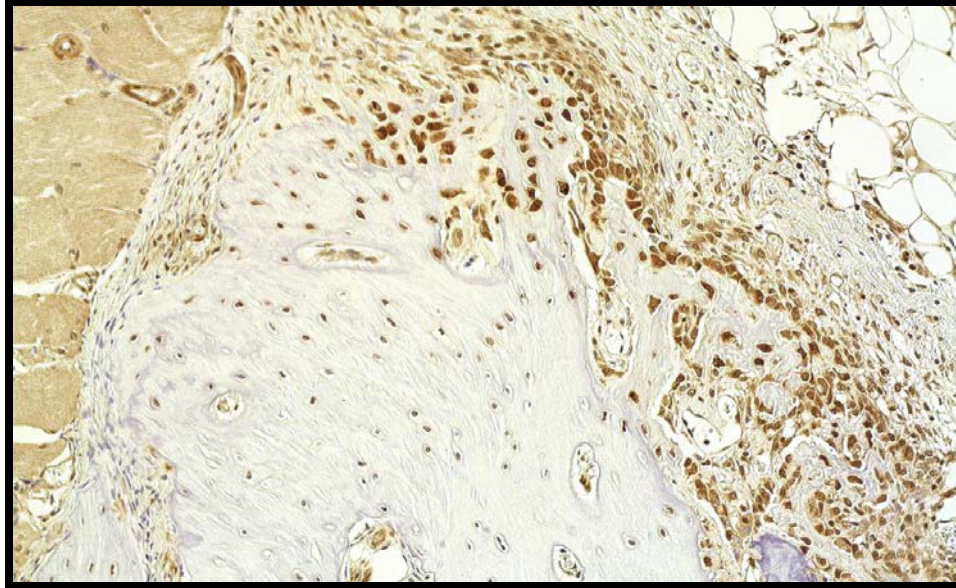


Figure 28: Msi1 Day5 20 μ g 5.84-13, 20x

Day #7

Msi1 expression of cells in the parietal ridge region peaked at day #7. Robust expression was evident within a thick band of connective tissue and osteoid running from the ridge eminence medially to the defect margin where it abruptly dropped off. Figure 29 offers one of the strongest indications that healing via differentiated osteo/fibroblastic stem cells in the parietal ridge region differs from the dura. Expression of Msi1 positive cells in the proliferating region superior to the dura mater is not observable.

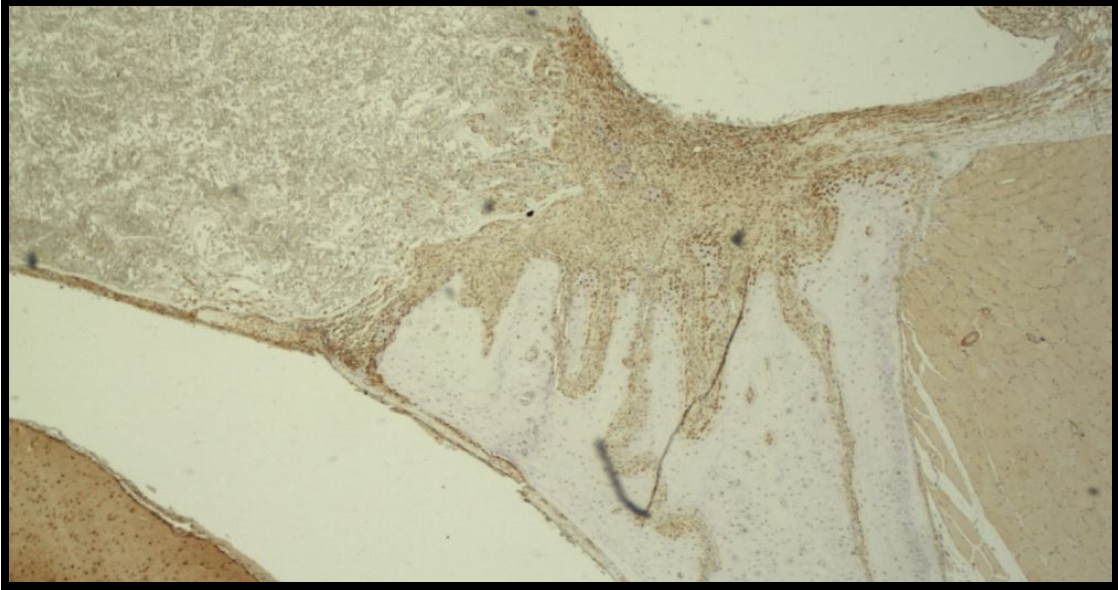


Figure 29: Msi1 Day7 0 μ g 7.110-8, 4x

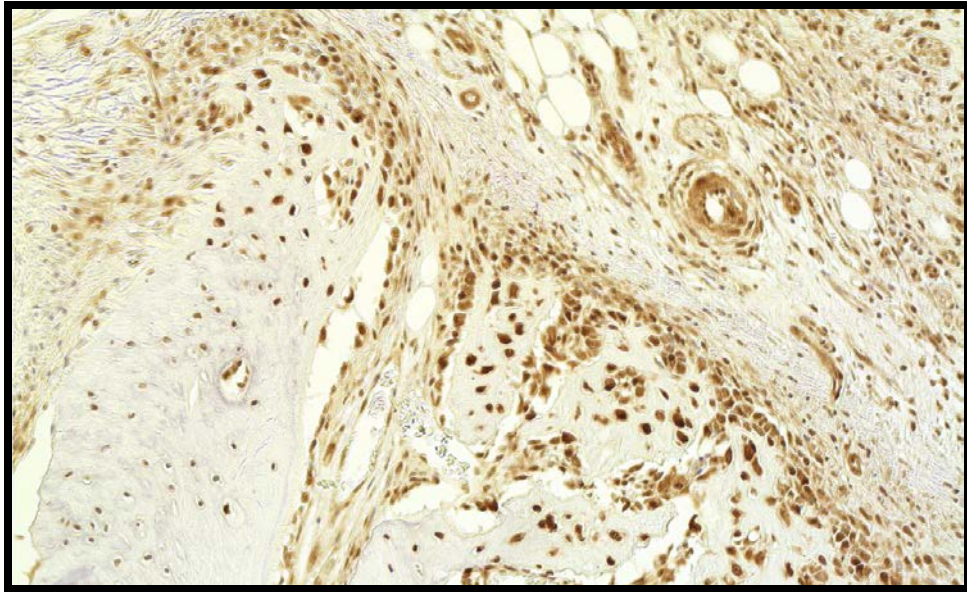


Figure 30: Msi1 Day7 5 μ g 7.111-6, 20x

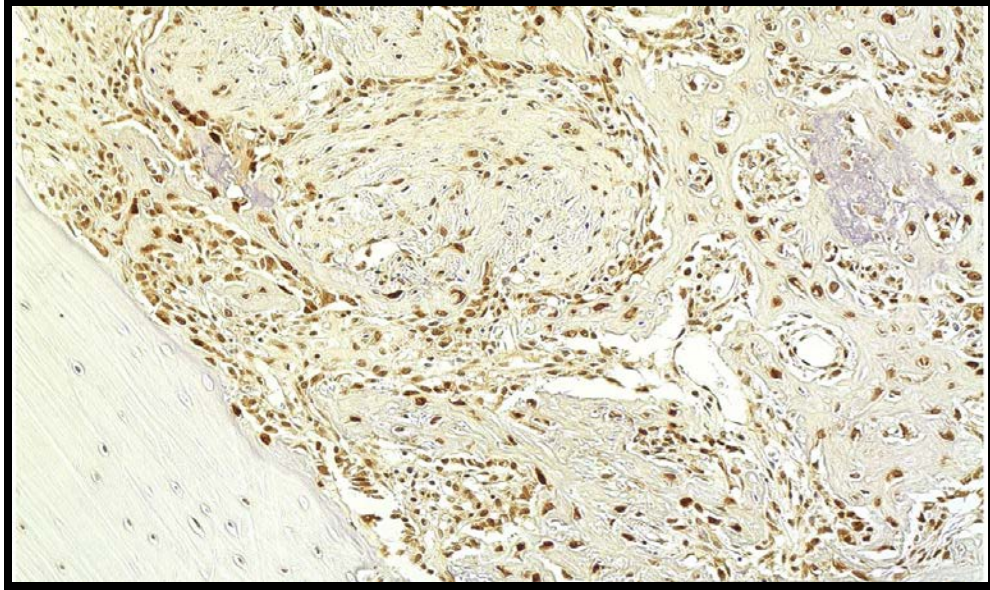


Figure 31: Msi1 Day7 20 μ g 7.133-14, 20x

Day #14

Musashi expression appeared to decrease at two weeks in the newly formed tissue regions medial to the parietal ridge. Heavily-stained, cuboidal cells were observed along the bone formation front but stellate cells further from the ridge did not exhibit activity levels that were seen at day #7. Osteocytes within the newly formed bone were positive for Msi1 and displayed heavily-stained, enlarged nuclei similar to those within the eminence region of the parietal ridge. This would be consistent with a cell lineage originating from the region of interest. Like KLF-4, Msi1 expression did not appear to correlate with levels of rhBMP-2.

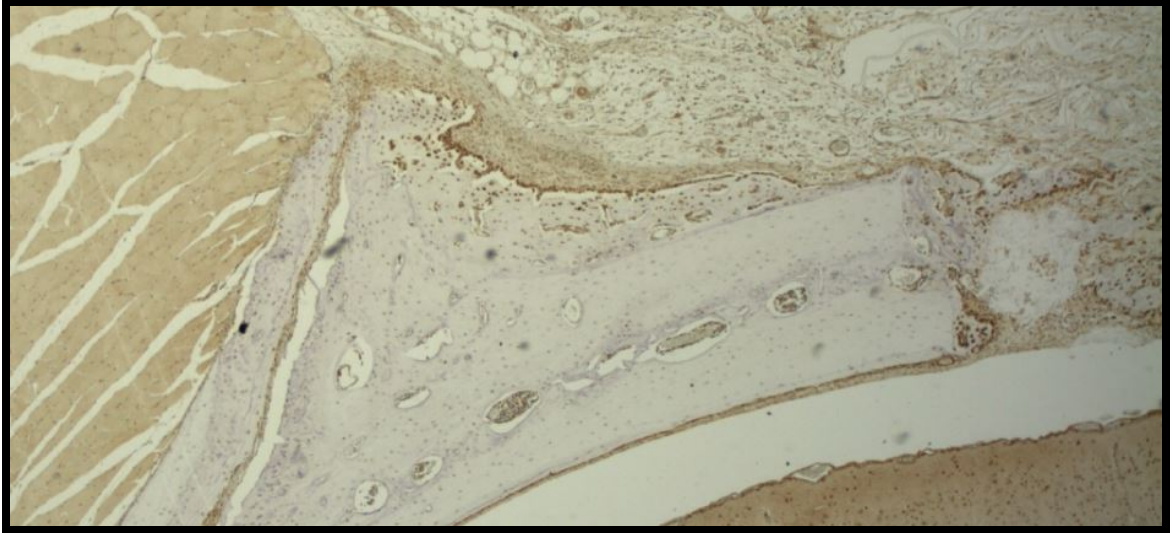


Figure 32: Msi1 Day14 0 μ g 14.61-12, 4x

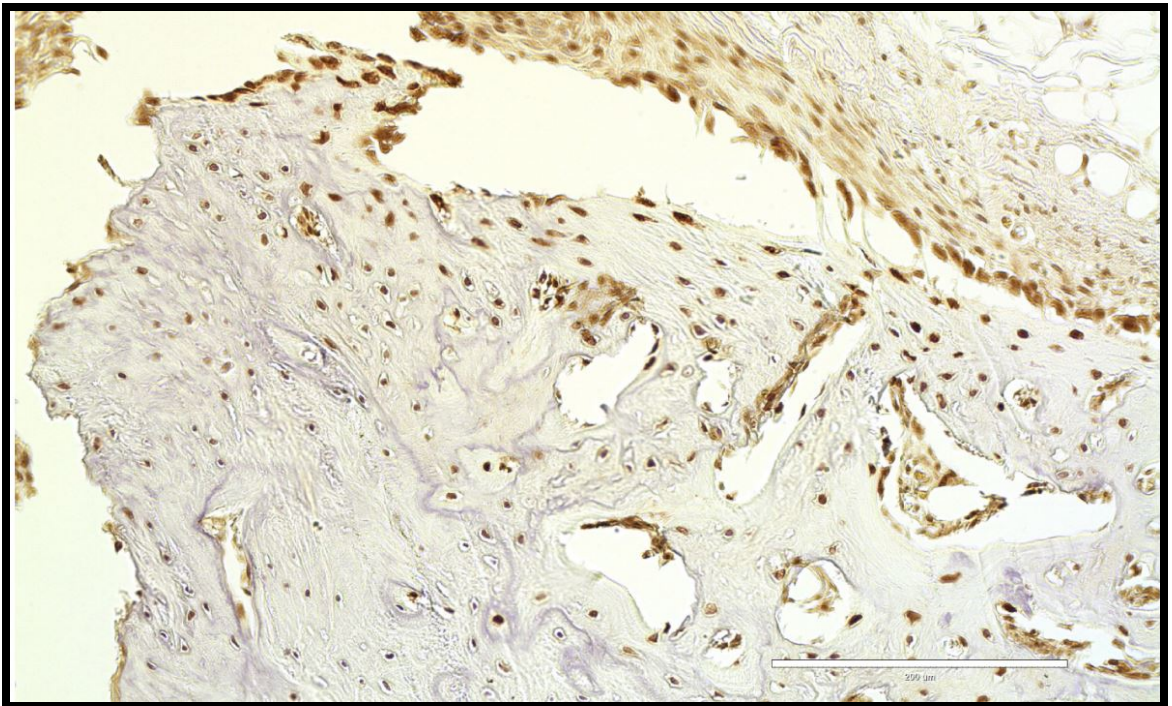


Figure 33: Msi1 Day14 5 μ g 14.65-9, 20x

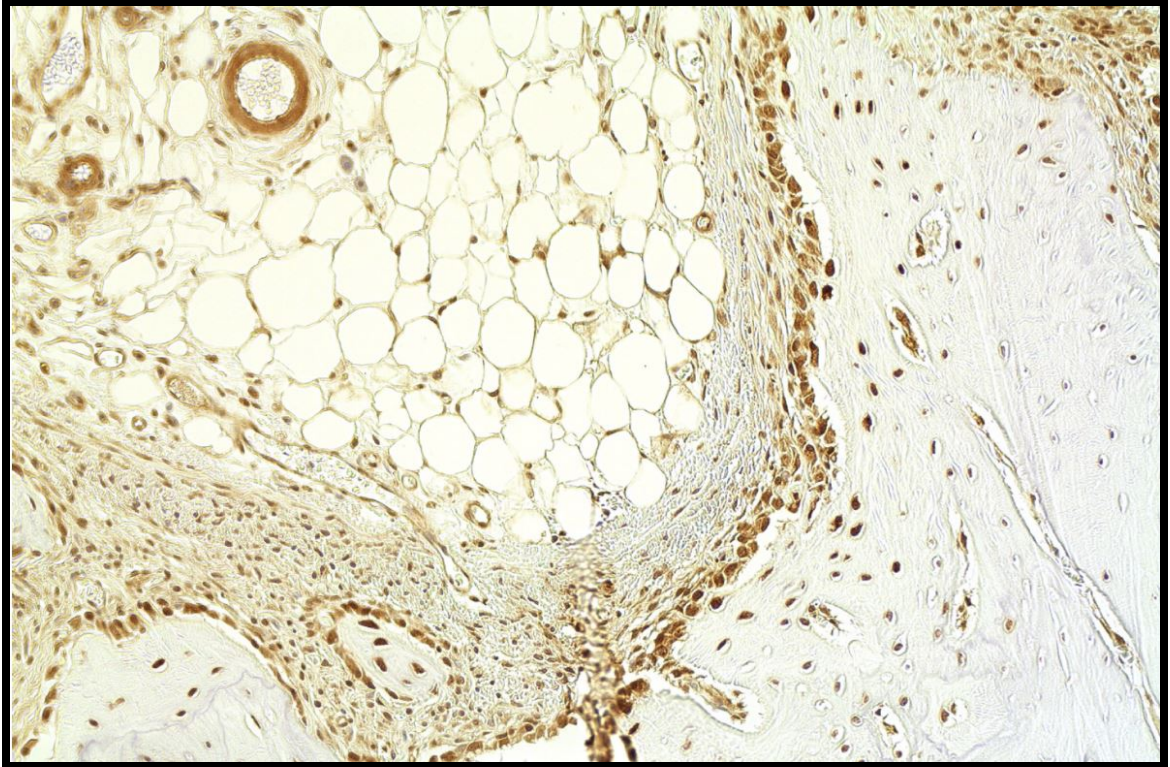


Figure 34: Msi1 Day14 20 μ g 14.62-5, 20x

Sex Determining Region Y-Box 2 (SOX-2)

Day #1-Day #14

SOX-2 expression was weak throughout all time points and rhBMP-2 concentrations. This signal responsible for maintaining the pluripotency of undifferentiated stem cells was not found in the area of high activity and new bone formation nor in areas inferior to the parietal ridge apex in which mesenchymal stem cells were not hypothesized to reside.

Select slides are shown to illustrate the negative pattern seen with SOX-2. However, SOX-2 expression was observed in the condylar and epidermal regions where stem cells are known to reside in an undifferentiated state. This serves as a positive control for the staining process used for this slide series.



Figure 35: SOX2 Day1 0 μ g 1.1-15, 4x

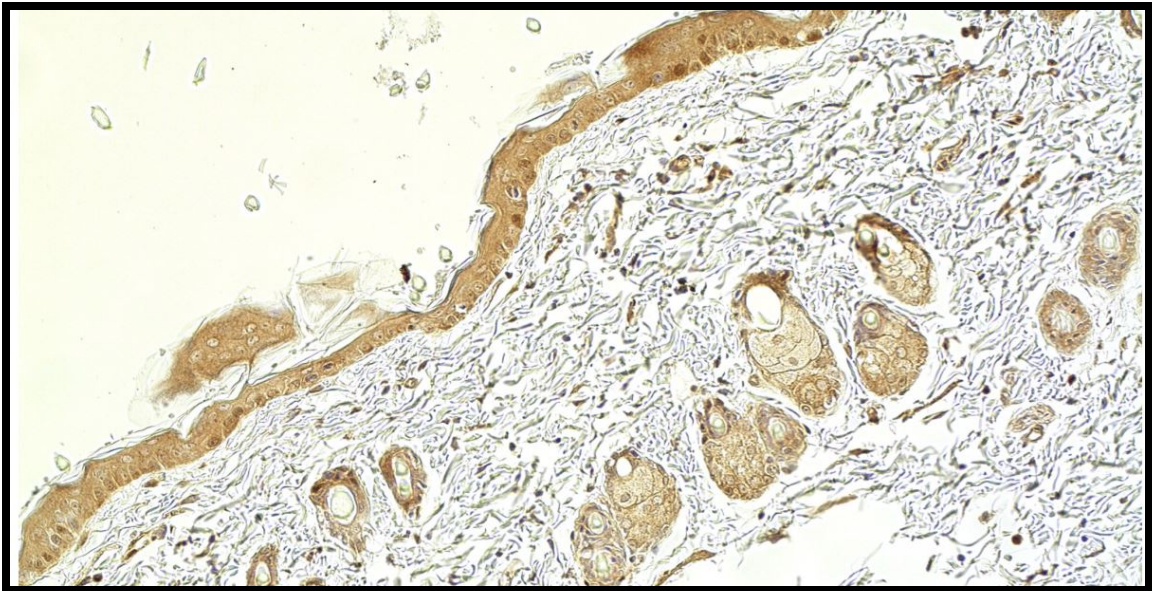


Figure 36 (Epidermis): SOX2 Day1 0 μ g 1.1-15, 20x

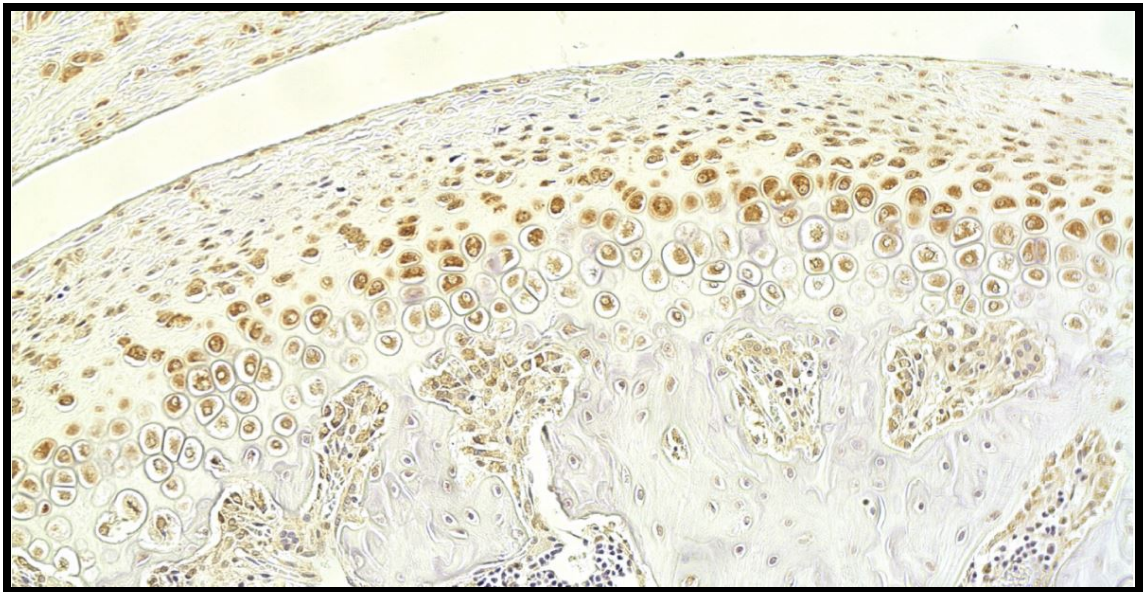
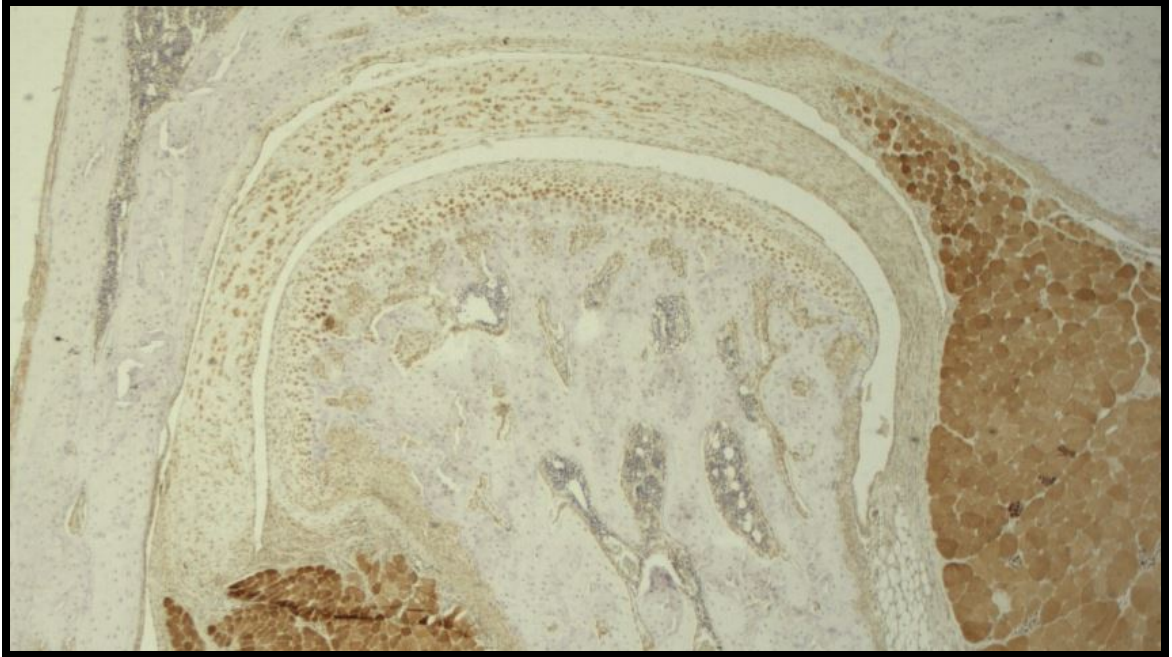


Figure 37a & b (Condyle): SOX2 Day 1 0 μ g 1.1-15, 20x



Figure 38: SOX2 Day1 0 μ g 1.1-15, 20x

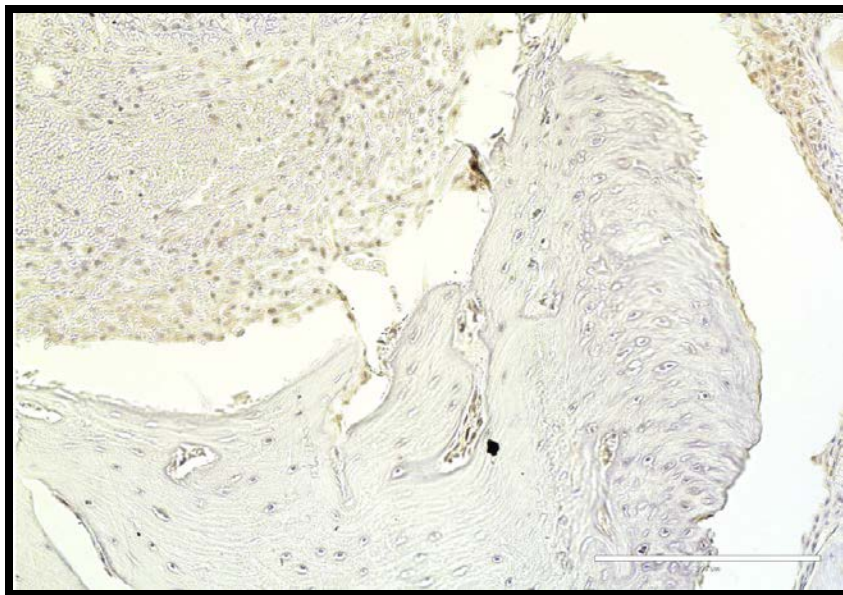


Figure 39: SOX2 Day3 0 μ g 3.46-6, 20x

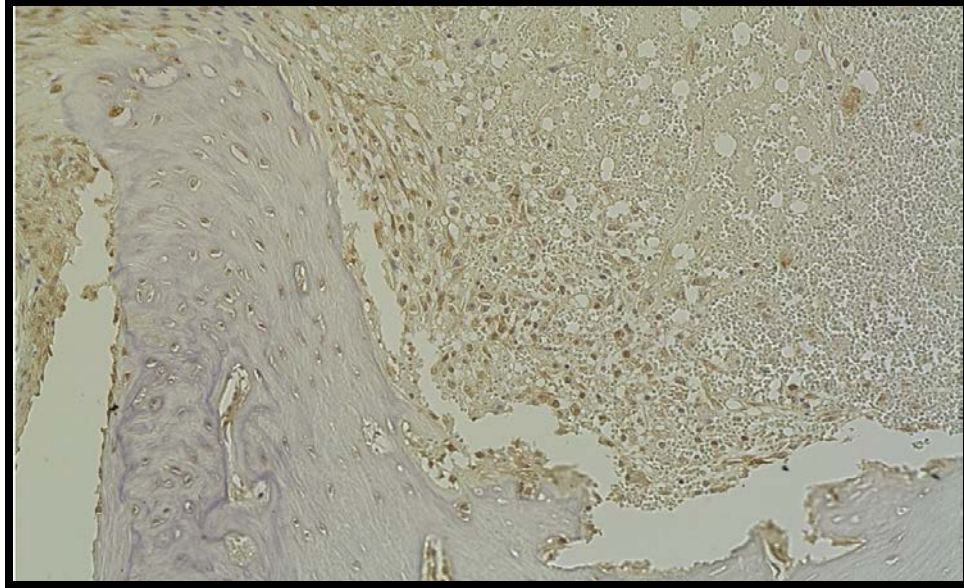


Figure 40: SOX2 Day3 20 μ g 3.45-5, 20x

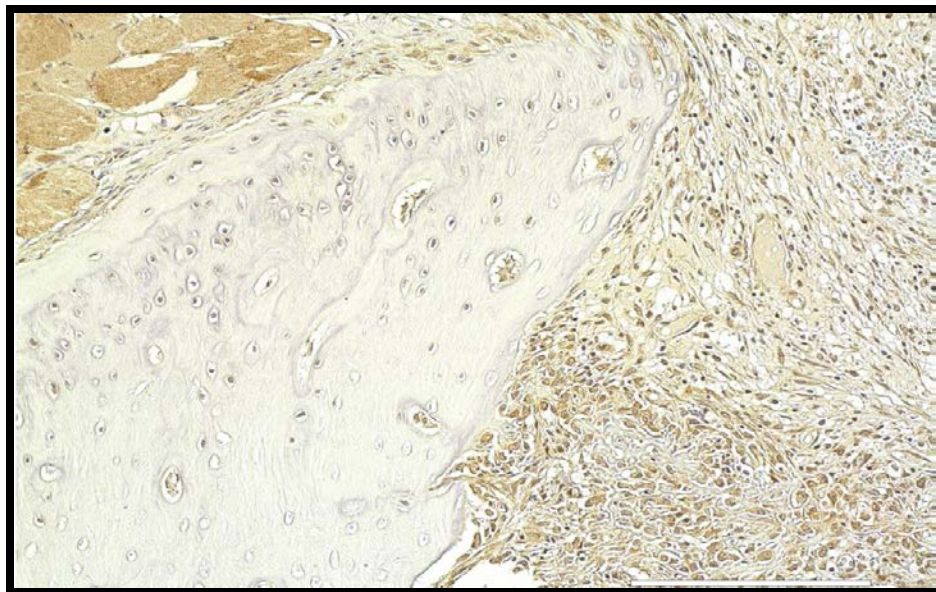


Figure 41: SOX2 Day7 0 μ g 7.131-3, 0 μ g 20x

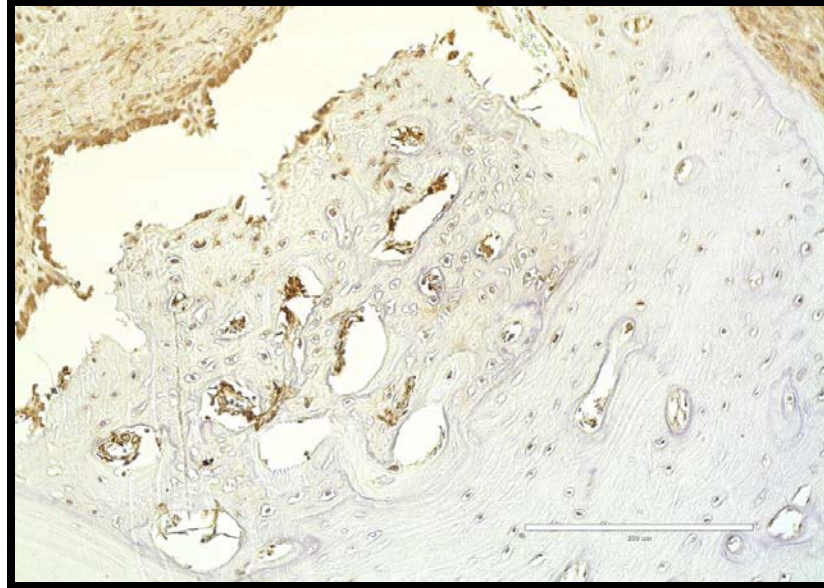


Figure 42: SOX2 Day14-5µg 14.59-2, 20x

Proliferating Cell Nuclear Antigen (PCNA)

Day #1-Day #14

PCNA results show high mitotic activity in the crestal bone eminence region and along the medial slope in the direction of the defect. Osteocytes in this region are weakly stained but do show a positive response compared to the negative pattern observed in the body of calvarial bone. Activity was strongest along areas of new bone formation and along the bone lining cells of the parietal ridge. PCNA activity did not exhibit a dose-response relationship to rhBMP-2 concentrations. A region of epidermis is included to serve as a positive control for PCNA staining. Basal regions within the epidermal layer as well as root of hair follicles exhibited the strongest staining patterns.

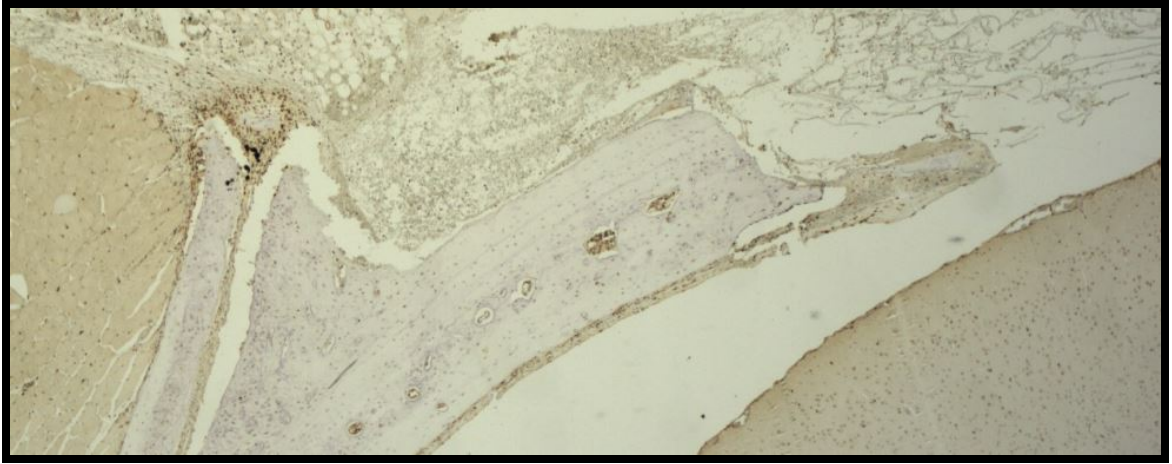


Figure 43: PCNA Day1 0 μ g 1.10-14 4x

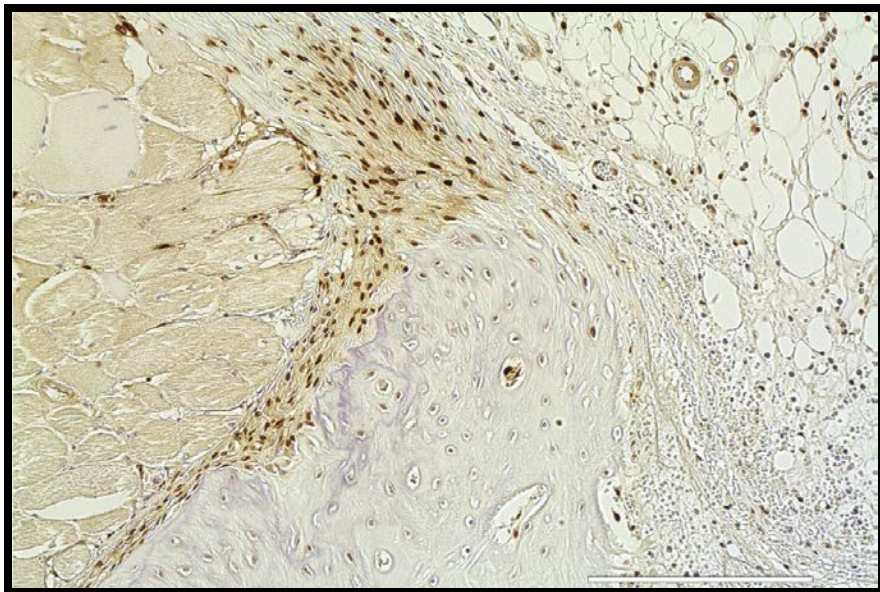


Figure 44: PCNA Day1 5 μ g 1.8-8 20x

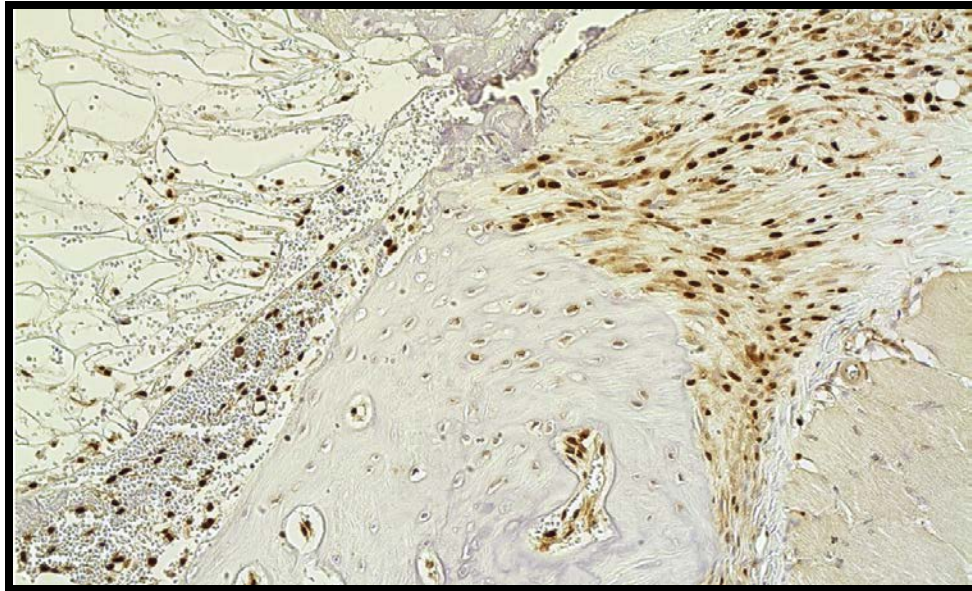


Figure 45: PCNA Day3 5 μ g 3.32-10 20x

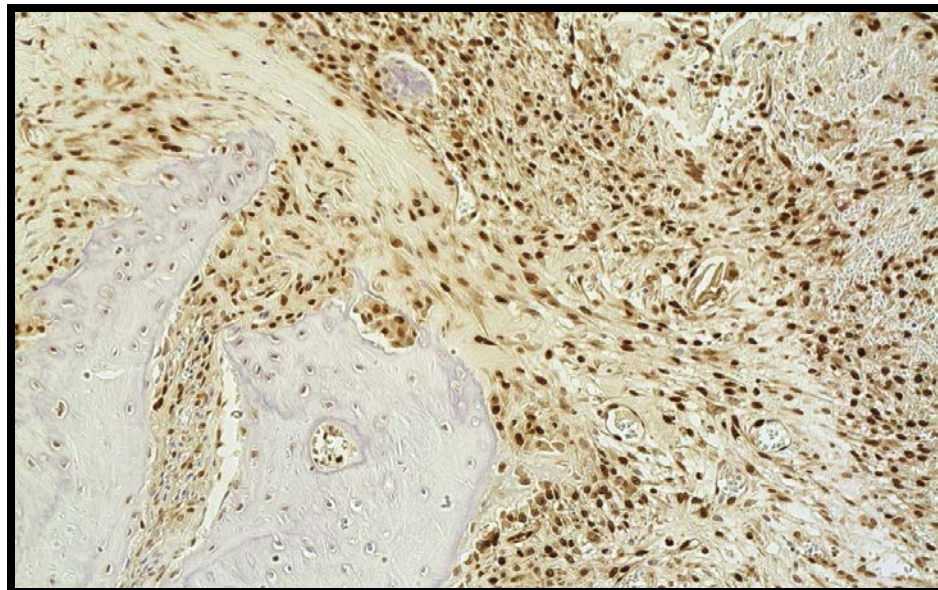


Figure 46: PCNA Day5 0 μ g 5.103-5 20x

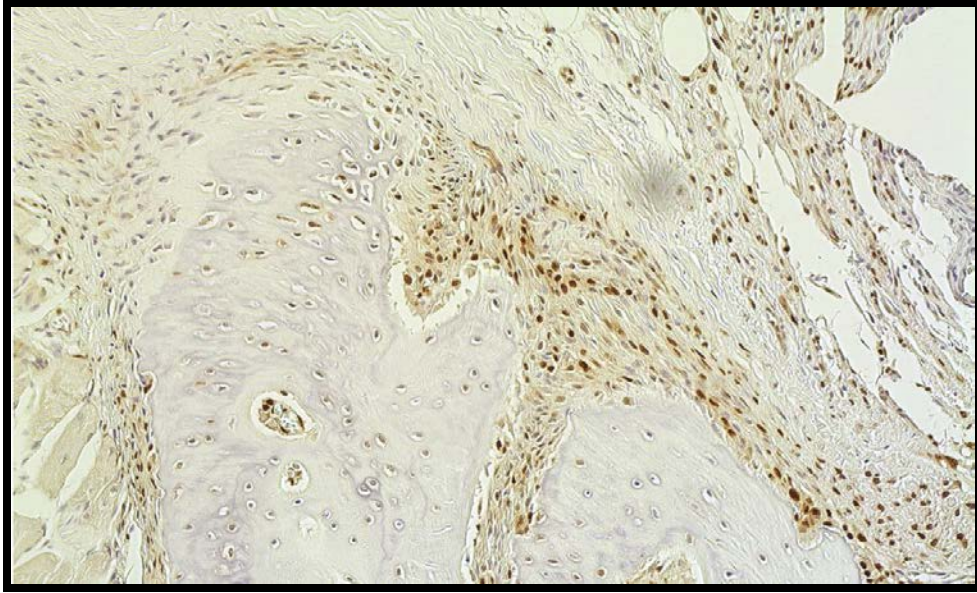


Figure 47: PCNA Day7 5 μ g 7.129-15 20x

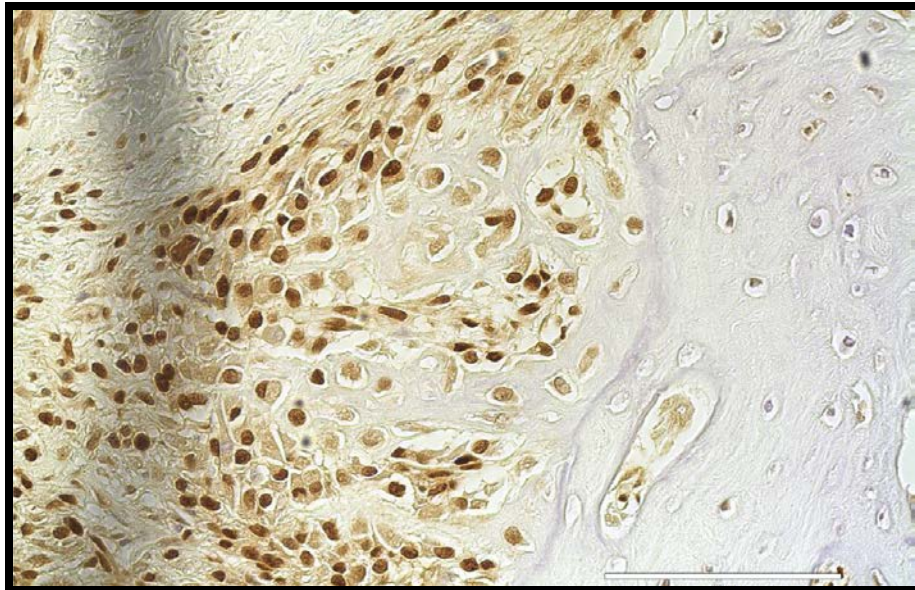


Figure 48: PCNA Day7 5 μ g 7.129-15 40x

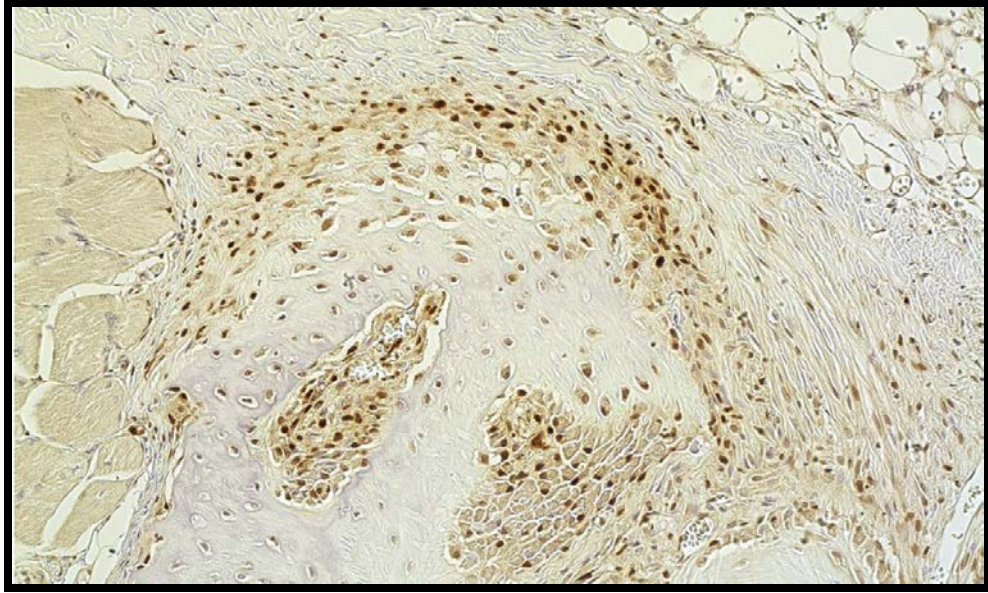


Figure 49: PCNA Day14 5 μ g 14.71-5 20x

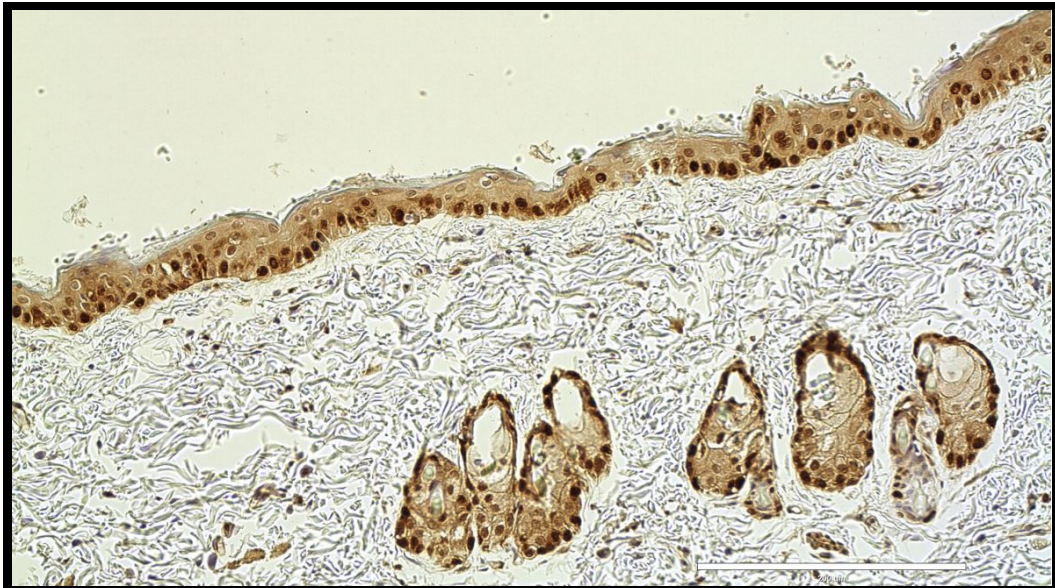


Figure 50: PCNA Day1 μ g 1.10-14 20x

Scleraxis Homolog A (SCXA)

Day #1-Day #14

Scleraxis expression was strong at the ridge eminence on day #1. Highly mitotic cells of the tendon insertion point showed a particularly robust response. Over the five time points, this signal decreased. The signal was not strong around areas where new bone formation had already occurred but rather was observed to be present in these areas at time points preceding the appearance of new bone. SCXA expression peaked at day #1 and #3 in the area of the tendon insertion point. Condylar expression was pronounced, consistent with SOX2 results. Similar to other antibody series, SCXA expression was unaffected by rhBMP-2 concentrations.

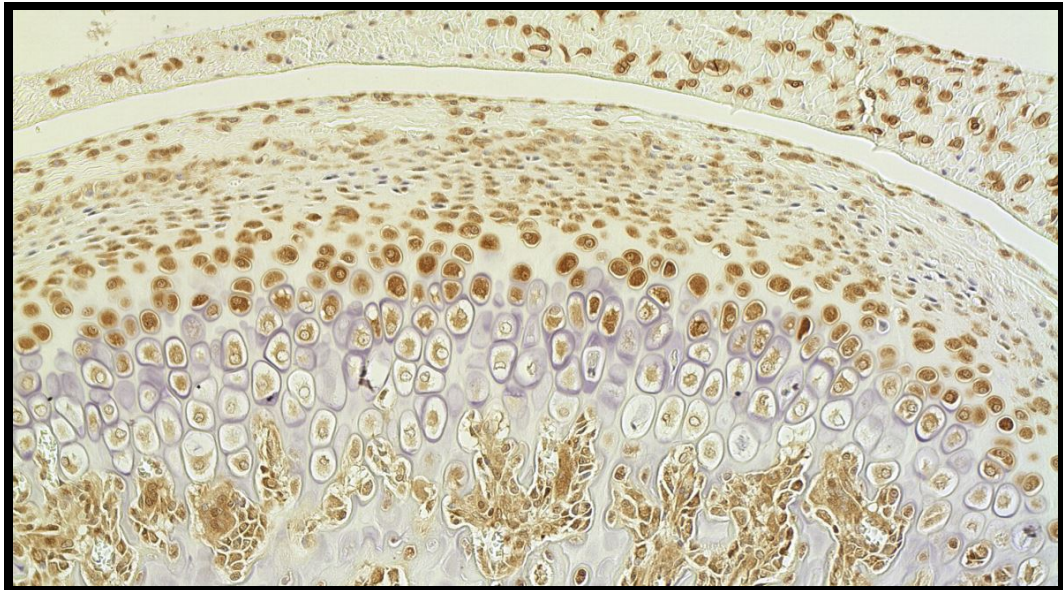


Figure 51 (Condyle): SCXA Day1 20 μ g 1,25-15, 20x

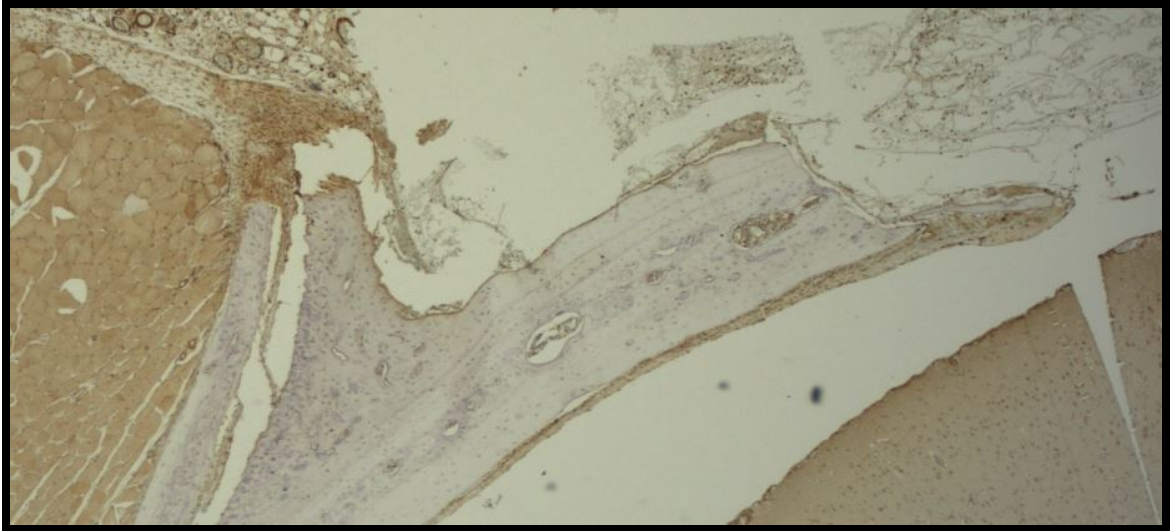


Figure 52: SCXA Day1 0μg 1.10-3

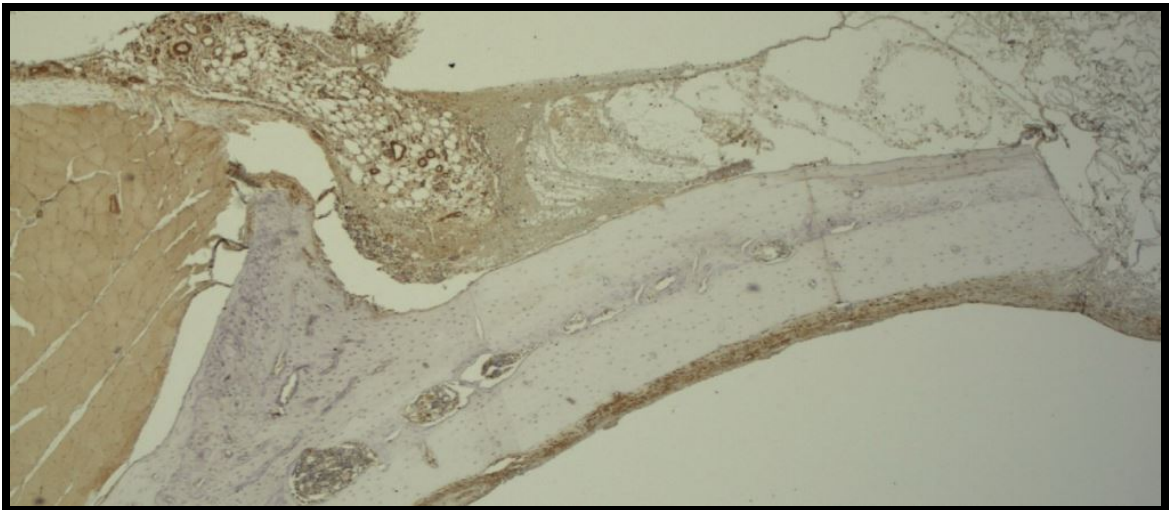


Figure 53: SCXA Day3 0μg 3.37-15, 4x

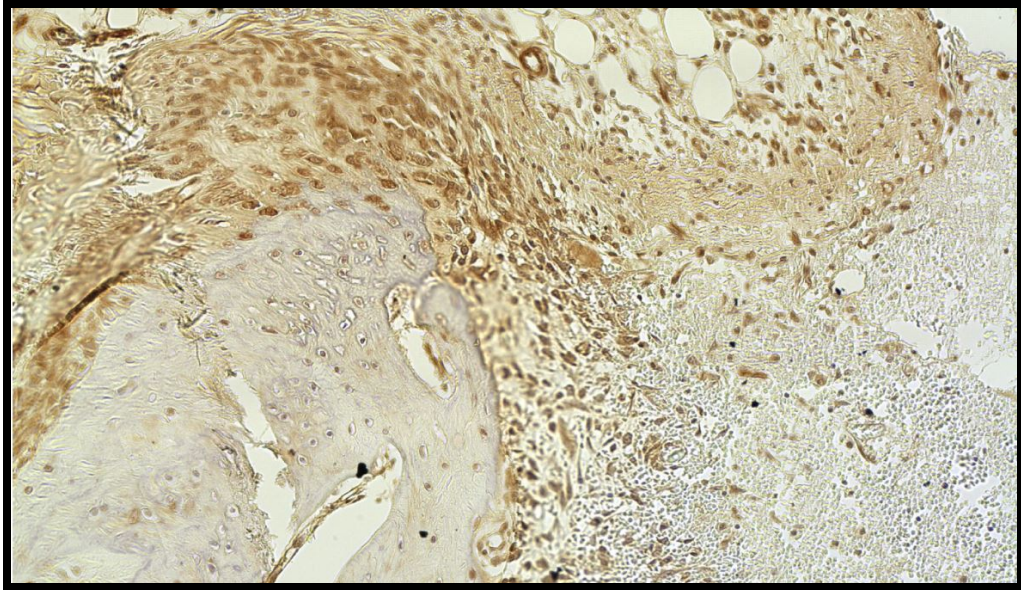


Figure 54: SCXA Day3 5µg 3.32-6, 20x

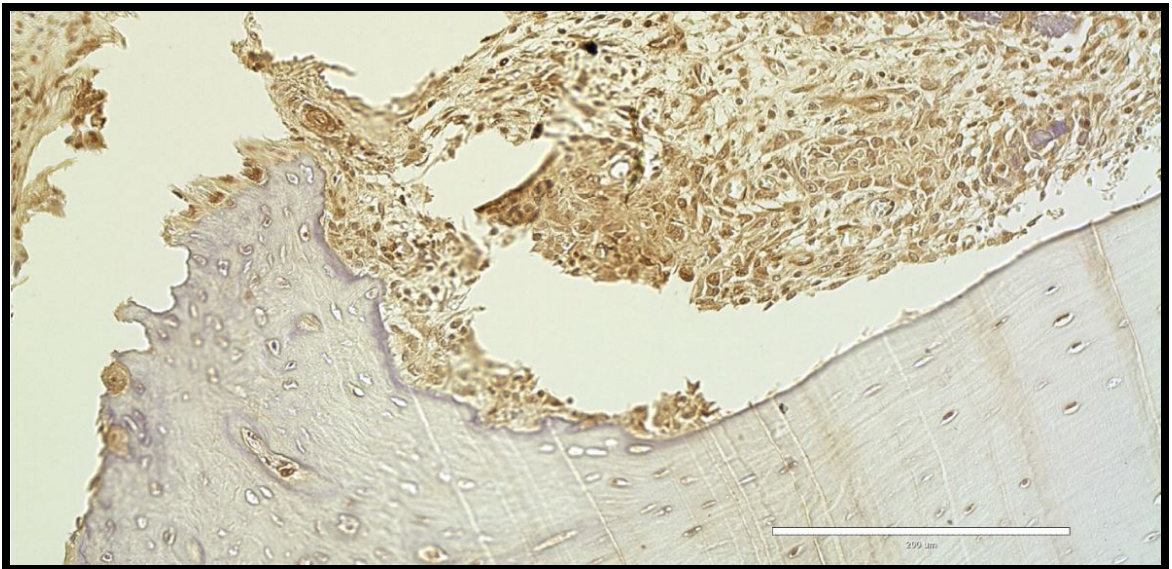


Figure 55: SCXA Day5 20µg 5.90-14, 20x

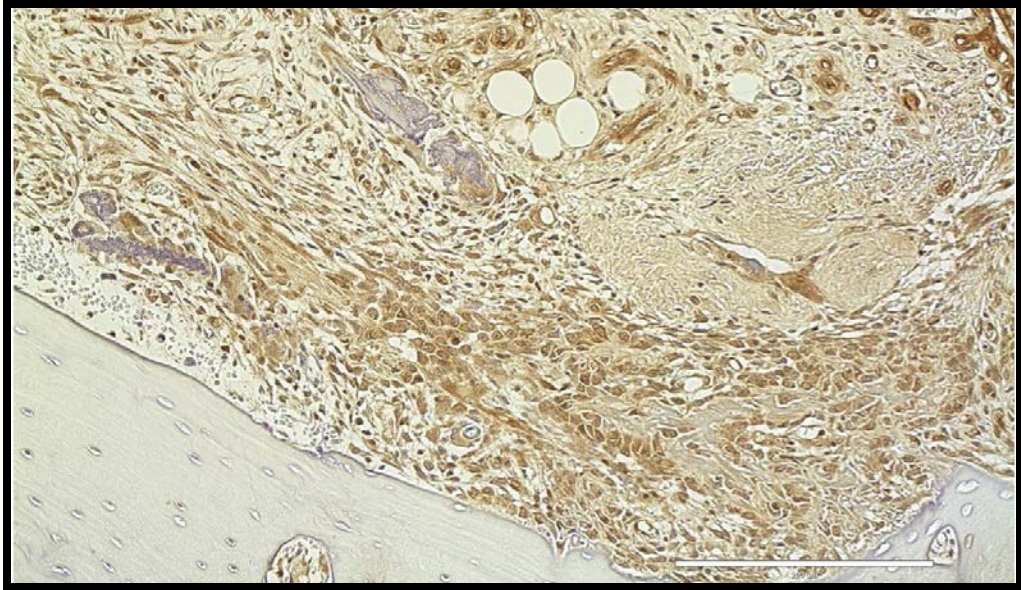


Figure 56: SCXA Day5 20 μ g 5.90-14, 20x

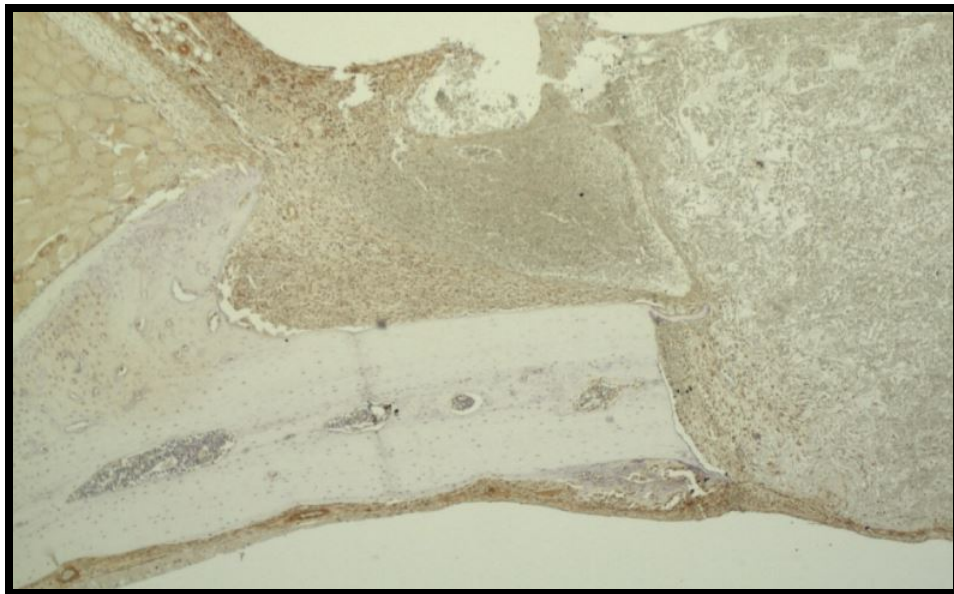


Figure 57: SCXA Day7 0 μ g 7.131-6, 4x

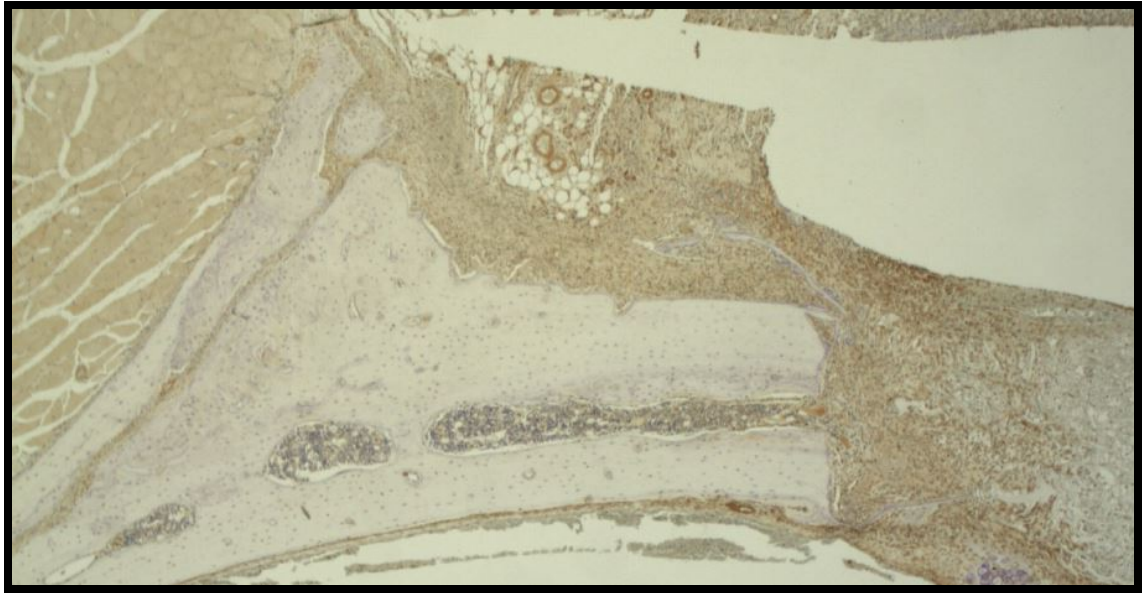


Figure 58: SCXA Day7 20µg 7.127-4, 4x

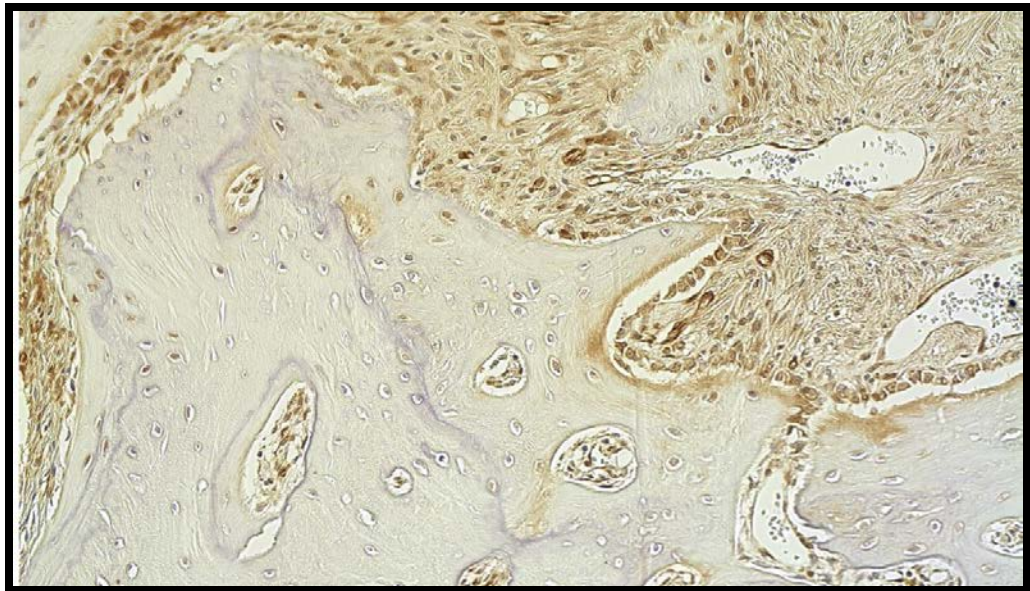


Figure 59: SCXA Day14 0µg 14.70-5, 20x

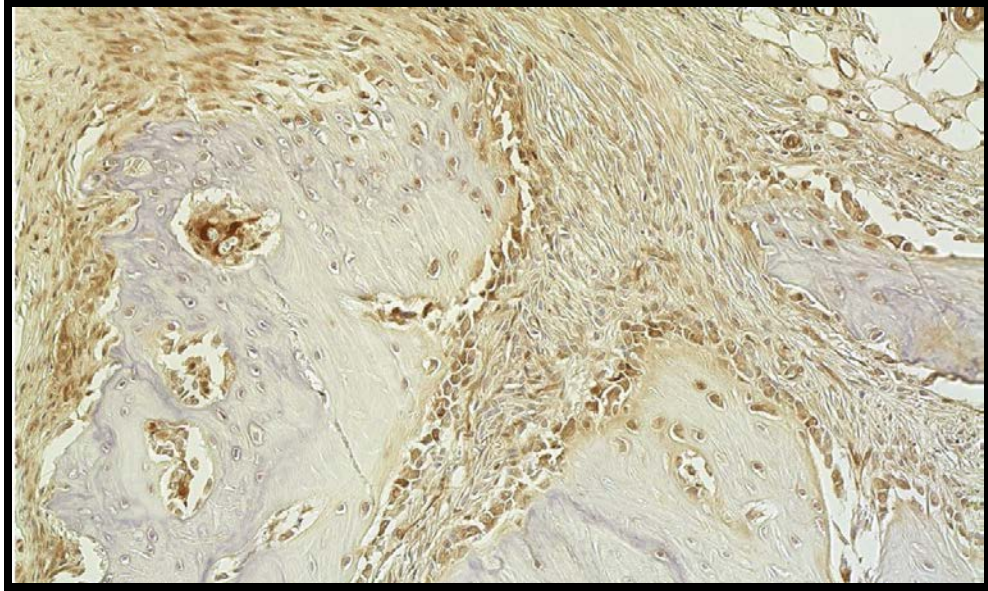


Figure 60: SCXA Day14 20 μ g 14.63-6, 20x

Sex Determining Region Y-Box 9 (SOX9)

SOX9 expression was not observed in the parietal ridge region at all time points and rhBMP-2 dosages. Expression present in the condyle region serves as a positive control for the staining series. Chondroblastic differentiation was observed in the dural region of the calvarial defect at day #7.

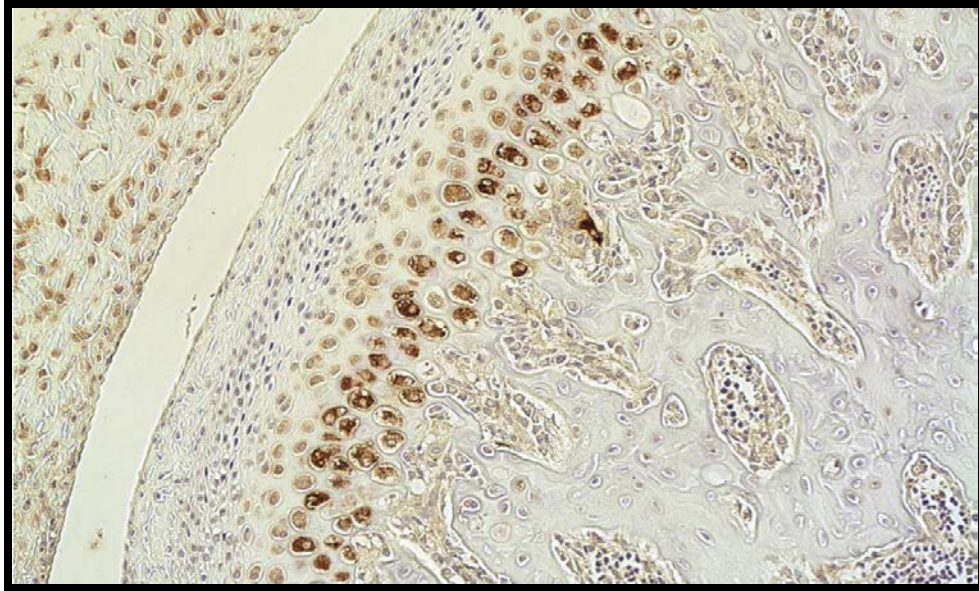


Figure 61: SOX9 Day1 20µg 1.25-10, 20x

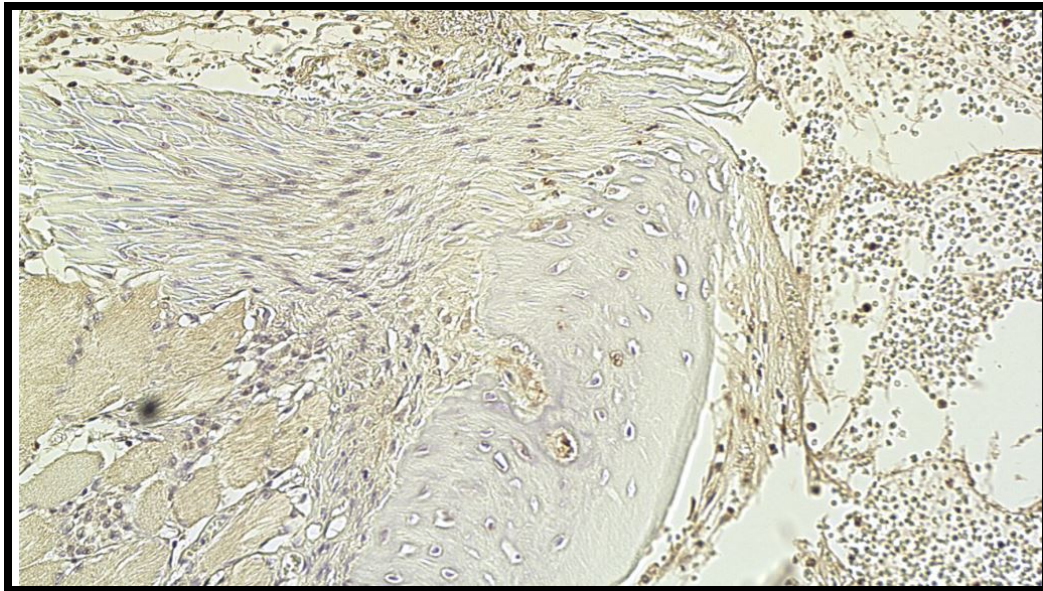


Figure 62: SOX9 Day1 20µg 1,25-10, 20x

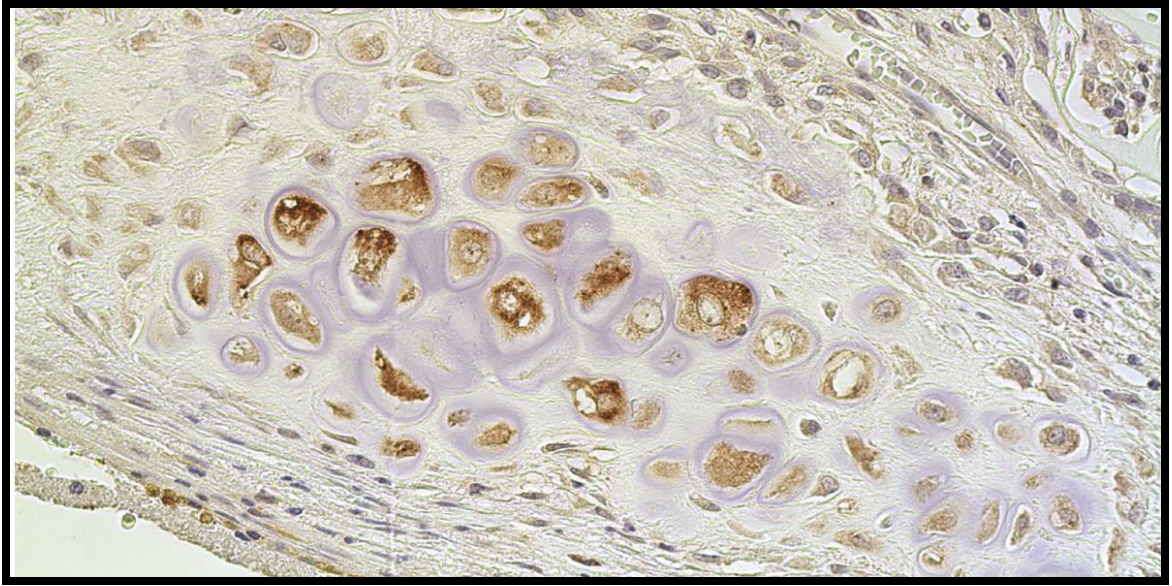


Figure 63 (Dura): SOX9 Day7 5 μ g 7,127-7, 40x

DISCUSSION

KLF-4 is valuable as both a marker of M2 macrophage polarization as well as pluripotent mesenchymal stem cells. A positive signal for KLF-4 expression in regions where osteoblastic differentiation potential is suspected would be consistent with the hypothesis that pluripotent stem cells exist in the area and are capable of differentiating along the osteoblast cell lineage.

In our staining series, KLF-4 expression was seen on day #1 only in immune cells. These were presumably M2 macrophages activated in the area by the creation of the calvarial defect. The cells of the parietal ridge were negative, which would be expected if their differentiation was only in the initial stages.

However, KLF-4 expression began to appear in the bone eminence at day #3 and gradually increased its intensity. This is consistent with PCNA results indicating high degrees of mitotic activity. These data would suggest that mesenchymal stem cells were activated by local signals to begin differentiation along their osteoblastic cell lineage.

Cellular activity observed in this antibody series did not seem to be affected by rhBMP-2 concentrations. This supports our hypothesis that there exists a population of mesenchymal stem cells in the parietal ridge region that are capable of differentiating along the osteoblastic cell lineage and do not respond to changes in local rhBMP-2 concentrations.

Msi1 is a mesenchymal stem cell marker which we hypothesized would be expressed by this subset of pluripotent stem cells in the parietal ridge. If expression were observed to differ from that of the cells within the dural region, it

would suggest a distinct subset of osteoblastic precursors. That is exactly what was observed in this staining series.

Large, heavily-stained nuclei were seen only in the superior-most region of the bone eminence in areas of high mitotic activity. No such expression was seen in osteocytes and bone-lining cells inferior to the parietal ridge. Additionally, significant expression of this marker was not seen in the dural regions, indicating it may play a different role there.

Expression peaked around day #7 with areas of high osteoblastic activity. This was located along the medial slope of the eminence between the ridge apex and the defect margin. This is consistent with osteoblastic differentiation originating from the parietal ridge tendon insertion point proliferating in response to tissue injury and initiating new bone formation during healing.

PCNA served as a comparative marker to support the hypothesis that osteoblastic stem cells were proliferating in the parietal ridge and not in nearby regions. As suspected, areas of high mitotic activity were observed near the tendon insertion point following creation of the surgical defect. Areas within the calvarial bone did not show mitotic activity which would be expected if mesenchymal stem cells were not present in this region or were not induced to differentiate in response to the injury. This is consistent with our hypothesis that mesenchymal stem cells exist in the parietal ridge and differentiate in response to local tissue injury.

High areas of mitotic activity were observed throughout the staining series along areas of new bone formation. Additionally, high areas of mitotic activity

were observed in the basal epidermal layers and hair follicles. Since these areas are known to express high basal levels of mitotic activity, these data served as a control, validating the results seen in our region of interest.

We expected that rhBMP-2 concentrations would have a general dose-response relationship with mitotic activity. However, this correlation was not observed in our staining series. This would be consistent with our hypothesis that rhBMP-2 is not a potent differentiation factor for mesenchymal stem cells in the parietal ridge.

Scleraxis A expression peaked early in the series and was observed to decrease over time. This tendon transcription factor was expected to be strongly expressed in the bone eminence region, consistent with its role as a tendon insertion point.

The expression of SCXA was observed to decrease substantially in areas of new bone formation which is consistent with our expectations, since these areas no longer serve as tendon insertion points but rather as newly regenerated woven bone. However, marked expression was seen in these same areas in earlier time points before the appearance of new bone, indicating it may serve a role in osteoblastic differentiation in this distinct population. Immunofluorescence would serve well here to quantify expression of SCXA over time to investigate its temporal role in this cell lineage.

SOX2 is known to serve a role in maintaining the pluripotency of stem cells latent within a region with regenerative potential. If a region were actively dividing and regenerating new bone, we would expect to see limited SOX2

expression if any at all. This is exactly what was observed in our slide series. Limited signal was present in the parietal ridge and in areas of new bone formation. This is consistent with our hypothesis that stem cells exist in this region and differentiate along the osteoblastic cell lineage in response to local tissue insult. If SOX2 expression were observed, it would suggest that stem cell differentiation was suppressed despite the creation of the surgical defect. Since strong expression was observed in the condylar region where osteoblastic/chondroblastic mesenchymal stem cells are known to exist, presence of this positive control provides confidence that negative expression seen in the parietal ridge is valid.

In addition to SOX2 data, negative expression of SOX9 within the parietal ridge supports the hypothesis that these mesenchymal stem cells differentiate along the osteoblastic cell lineage rather than chondroblastic cell lineage.

Due to limitations in time and resources, hypothesis #2 concerning the effects of hypoxia on osteoblastic differentiation in the region of interest was not pursued. Additionally, individual macrophage regenerative proteins present in response to local tissue damage was not pursued.

Immunofluorescence was not pursued due to similar limitations. Quantification of these data would have been the next step in order to elucidate the role these various transcription factors play throughout the timeframe examined.

FUTURE STUDIES

Mesenchymal stem cells of the parietal ridge have been observed to respond differently to osteoblastic differentiation proteins when compared to their counterparts in the dura mater. Identification of the exact nature of this difference would allow us to look for these distinct populations of cells in other tendon insertion points (e.g. periodontal ligament). If these cells are identified and their differentiation factors well understood, it is possible that their reparative capabilities could be exploited to enhance periodontal regeneration. Our study supported the hypothesis that bone morphogenetic protein-2 was not a potent differentiation factor for this distinct population. Future studies could focus on testing other possible targets.

REFERENCES

1. Berendsen AD, Olsen BR. Bone development. *Bone*. 2015;80:14-18.
2. Blitz E, Sharir A, Akiyama H, Zelzer E. Tendon-bone attachment unit is formed modularly by a distinct pool of Scx- and Sox9-positive progenitors. *Development*. 2013;140(13):2680-2690.
3. Burke D, Dishowitz M, Sweetwyne M, Miedel E, Hankenson KD, Kelly DJ. The role of oxygen as a regulator of stem cell fate during fracture repair in TSP2-null mice. *Journal of Orthopaedic Research*. 2013;31(10):1585-1596.
4. Chambers, TJ, Horton MA. Failure of cells of the mononuclear phagocyte series to resorb bone. *Calcif Tissue Int* 1984; 36: 556-558
5. Chenard KE, Teven CM, He T, Reid RR. Bone morphogenetic proteins in craniofacial surgery: current techniques, clinical experiences, and the future of personalized stem cell therapy. *J Biomed Biotechnol*. 2012;2012:601549-601549.
6. Colnot C. Skeletal Cell Fate Decisions Within Periosteum and Bone Marrow During Bone Regeneration. *Journal of Bone and Mineral Research*. 2009;24(2):274-282.
7. Coons AH, Creech HJ, and Jones RN: Immunological properties of an antibody containing a fluorescent group. *Proc Soc Exp Biol Med* 1941; 47: pp. 200
8. Dabbs, David J., MD. "Techniques of Immunohistochemistry: Principles, Pitfalls and Standardization." *Diagnostic Immunohistochemistry: Theranostic and Genomic Applications*. 4th ed. N.p.: Saunders, n.d. 9-10. Print.
9. Das R., Jahr H., van Osch G. J. V. M., Farrell E. The role of hypoxia in bone marrow-derived mesenchymal stem cells: considerations for regenerative medicine approaches. *Tissue Engineering—Part B: Reviews*. 2010;16(2):159–168.

10. DeCardona, E. *Bone Morphogenic Protein-2 Kinetics and Target Signaling Pathways During Bone Regeneration in a Rat Critical-Sized Calvarial Defect Model*. Thesis, 2015. Georgia Regents University.
11. Eming SA, Krieg T, and Davidson JM "Inflammation in Wound Repair: Molecular and Cellular Mechanisms" *Journal of Investigative Dermatology* 2007; 127:514-525
12. Fritschy, Jean-Marc, and Härtig, Wolfgang (Apr 2001) Immunofluorescence. In: eLS. John Wiley & Sons Ltd, Chichester. <http://www.els.net>
13. Galli SJ, Borregaard N, Wynn TA. Phenotypic and functional plasticity of cells of innate immunity: macrophages, mast cells and neutrophils. *Nature immunology*. 2011;12(11):1035-1044.
14. Gartner, L. & Hiatt, J. 2007, *Color Textbook of Histology*, 3rd edn, Saunders, Philadelphia.
15. Huang LE, Arany Z, Livingston DM, Bunn HF. Activation of Hypoxia-inducible Transcription Factor Depends Primarily upon Redox-sensitive Stabilization of Its α Subunit. *Journal of Biological Chemistry*. 1996;271(50):32253-32259.
16. Jusino M. *Role of Gas Molecule Signaling in Bone Morphogenetic Protein-2 Mediated Bone Regeneration in a Critical-Sized Rat Calvarial Defect Model*. Thesis, 2015. Georgia Regents University.
17. Kallio PJ, Pongratz I, Gradin K, McGuire J, Poellinger L (May 1997). "Activation of hypoxia-inducible factor 1 α : posttranscriptional regulation and conformational change by recruitment of the Arnt transcription factor". *Proceedings of the National Academy of Sciences of the United States of America*. **94** (11): 5667–72.
18. Kawaguchi, S. Unpublished.
19. Keith B, Simon MC. Hypoxia-Inducible Factors, Stem Cells, and Cancer. *Cell*. 2007;129(3):465-472.

20. Kumar, Vinay, Abul K. Abbas, Nelson Fausto, Stanley L. Robbins, and Ramzi S. Cotran. *Robbins and Cotran Pathologic Basis of Disease*. Philadelphia: Elsevier Saunders, 2005.
21. Liao X, Sharma N, Kapadia F, et al. Krüppel-like factor 4 regulates macrophage polarization. *J Clin Invest*. 2011;121(7):2736-2749.
22. Liu F, Malaval L, Aubin JE. The Mature Osteoblast Phenotype Is Characterized by Extensive Plasticity. *Exp Cell Res*. 1997;232(1):97-105.
23. Long, F. 2012, "Building strong bones: molecular regulation of the osteoblast lineage", *Nature reviews. Molecular cell biology*, vol. 13, no. 1, pp. 27-38.
24. Luzzani, C., Neiman, G., Garate, X., Questa, M., Solari, C., Fernandez Espinosa, D., Garc a, M., Errecalde, A.L., Guberman, A., Scassa, M.E., Sevlever, G.E., Romorini, L. & Miriuka, S.G. 2015, "A therapy-grade protocol for differentiation of pluripotent stem cells into mesenchymal stem cells using platelet lysate as supplement", *Stem Cell Research & Therapy*, vol. 6, no. 1, pp. 6.
25. Mackie EJ, Tatarczuch L, Mirams M. The skeleton: a multi-functional complex organ. The growth plate chondrocyte and endochondral ossification. *Journal of Endocrinology*. 2011;211(2):109-121.
26. Marynka-Kalmani, K., Treves, S., Yafee, M., Rachima, H., Gafni, Y., Cohen, M.A. & Pitaru, S. 2010, "The Lamina Propria of Adult Human Oral Mucosa Harbors a Novel Stem Cell Population", *STEM CELLS*, vol. 28, no. 5, pp. 984-995.
27. Miller SC, Jee WSS. The bone lining cell: A distinct phenotype?. *Calcif Tissue Int*. 1987;41(1):1-5.
28. O'Bryhim, J. *Effects of Bone Morphogenetic Protein-2 (BMP-2) on Initial Cellular Events in the Critical-Sized Rat Calvarial Defect Model: Focus on (Pre)Osteoblasts*. Thesis, 2015. Georgia Regents University.
29. Pelaez M, Susin C, Lee J, et al. Effect of rhBMP-2 dose on bone formation/maturation in a rat critical-size calvarial defect model. *J Clin Periodontol*. 2014;41(8):827-836.

30. Salim, A., Nacamuli, R.P., Morgan, E.F., Giaccia, A.J. & Longaker, M.T. 2004, "Transient Changes in Oxygen Tension Inhibit Osteogenic Differentiation and Runx2 Expression in Osteoblasts", *Journal of Biological Chemistry*, vol. 279, no. 38, pp. 40007-40016.
31. Sethi RKV, Kozin ED, Lee DJ, Shrime MG, Gray ST. Epidemiological Survey of Head and Neck Injuries and Trauma in the United States. *Otolaryngology--head and neck surgery : official journal of American Academy of Otolaryngology-Head and Neck Surgery*. 2014;151(5):776-784.
32. Shenaq, Deana S. et al. "Characterization of Reversibly Immortalized Calvarial Mesenchymal Progenitor Cells." *The Journal of craniofacial surgery* 26.4 (2015): 1207–1213. *PMC*. Web. 21 Aug. 2016.
33. Stiers P, van Gastel N, Carmeliet G. Targeting the hypoxic response in bone tissue engineering: A balance between supply and consumption to improve bone regeneration. *Mol Cell Endocrinol*. 2016;432:96-105.
34. Wingerd B. Muscles of the Head. In: *Rat Dissection Manual*. Illustrated ed. Baltimore and London: JHU Press, 1988; 1988:19.
35. Zelzer E, Blitz E, Killian ML, Thomopoulos S. Tendon-to-bone attachment: From development to maturity. *Birth Defects Research Part C: Embryo Today: Reviews*. 2014;102(1):101-112.